Landscape-level terrestrial methane flux observed from a very tall tower

Ankur R Desai[1*], Ke Xu[1], Hanqin Tian[2], Peter Weishampel[3], Jonathan Thom[1], Dan Baumann[4], Arlyn E. Andrews[5], Bruce D. Cook[6], Jennifer Y. King[7], Randall Kolka[8]

[1] Center for Climatic Research, University of Wisconsin-Madison, Madison, WI USA
[2] International Center for Climate and Global Change Research, Auburn University, Auburn, AL USA
[3] Great Lakes Domain, National Ecological Observatory Network, Inc., Land O Lakes, WI USA
[4] Wisconsin Water Science Center, U.S. Geological Survey, Rhinelander, WI USA
[5] Earth Systems Research Lab, National Oceanographic and Atmospheric Administration, Boulder, CO USA
[6] Goddard Space Flight Center, National Aeronautics and Space Administration, Greenbelt, MD USA
[7] Department of Geography, University of California, Santa Barbara, CA, USA
[8] USDA Forest Service Northern Research Station, Grand Rapids, MN USA

[*] Corresponding author: Ankur R Desai, Dept of Atmospheric and Oceanic Sciences, UW-Madison, 1225 W Dayton St, Madison, WI 53706 USA, desai@aos.wisc.edu, +1-608-218-4208

Abstract

Simulating the magnitude and variability of terrestrial methane sources and sinks poses a challenge to ecosystem models because the biophysical and biogeochemical processes that lead to methane emissions from terrestrial and freshwater ecosystems are, by their nature, episodic and spatially disjunct. As a consequence, model predictions of regional methane emissions based on field campaigns from short eddy covariance towers or static chambers have large uncertainties, because measurements focused on a particular known source of methane emission will be biased compared to regional estimates with regards to magnitude, spatial scale, or frequency of these emissions. Given the relatively large importance of predicting future terrestrial methane fluxes for constraining future atmospheric methane growth rates, a clear need exists to reduce spatiotemporal uncertainties. In 2010, an Ameriflux tower (US-PFa) near Park Falls, WI, USA, was instrumented with closed-path methane flux measurements at 122 m above ground in a mixed wetland-upland landscape representative of the Great Lakes region. Two years of flux observations revealed an average annual methane (CH_4) efflux of 785 +/- 75 mg C-CH_4 m^{-2} yr^{-1}, compared to a mean CO_2 sink of -80 g C-CO_2 m^{-2} yr^{-1}, a ratio of 1% in magnitude on a mole basis. Interannual variability in methane flux was 30% of the mean flux and driven by suppression of methane emissions during dry conditions in late summer 2012. Though relatively small, the magnitude of the methane source from the very tall tower measurements was mostly within the range previously measured using static chambers at nearby wetlands, but larger than a simple scaling of those fluxes to the tower footprint. . Seasonal patterns in methane fluxes are similar to those simulated in the Dynamic Land Ecosystem Model (DLEM), but magnitude depends on model parameterization and input data, especially regarding wetland extent. The model was unable to simulate short-term (sub-weekly) variability. Temperature was found to be a stronger driver of regional CH_4 flux than moisture availability or net ecosystem production at the daily to monthly scale. Taken together, these results emphasize the multi-timescale dependence of drivers of regional methane flux and the importance of long, continuous time series for their characterization.

Keywords: methane; eddy covariance; regional flux; land-atmosphere

1. Introduction

The contribution of microbial methane (CH_4) from wetlands remains a significant source of uncertainty in closing the global methane budget (Mikaloff Fletcher *et al.*, 2004). In particular, wetland methane emissions may contribute as much as 25-40% of global CH_4 anthropogenic emissions and are the leading source of interannual variability in atmospheric CH_4 (Bousquet *et al.*, 2006; Chen and Prinn, 2006; Crill *et al.*, 1993). The recent increase in the growth rate of atmospheric CH_4 lends particular urgency to improving global simulations and inversions of the terrestrial methane source (Chen and Prinn, 2006; Collins *et al.*, 2006). One set of hypothesized mechanisms is the role of warming of high latitudes and wetting of the tropics (Dlugokencky *et al.*, 2009). Because CH_4 emissions are closely linked to changes in regional hydrology and temperature, and ongoing climate changes are likely to have a significant impact on regional water tables and wetland soil temperatures, there is a high likelihood that climate change will affect wetland CH_4 emissions (Roulet *et al.*, 1992; Sulman *et al.*, 2009).

Model results provide motivation for long-term *in situ* observations of terrestrial CH_4 sources and sinks. However, virtually all *in situ* measurements of surface to atmosphere CH_4 flux have been conducted either at the plot scale, typically with chamber-based measurements (e.g., Jungkunst and Fiedler, 2007), or more recently at the ecosystem scale, particularly with eddy covariance flux towers (e.g., Hatala *et al.*, 2012). In contrast, atmospheric tracer-transport inversions (e.g., Bergamaschi *et al.*, 2010; Miller *et al.*, 2013), global ecosystem models (e.g,. Matthews and Fung, 1987; Tang *et al.*, 2010; Tian *et al.*, 2010), and global remote sensing based estimates of CH_4 sources (e.g., Bloom *et al.*, 2010) are provided at much larger spatial scales.

79 Consequently, a scale mismatch arises for evaluation across methods. This scale
80 mismatch is particularly difficult for CH_4 because of fine-scale spatial heterogeneity of
81 CH_4 sources and sinks and sampling biases toward known CH_4 sources (e.g. peatlands).
82 The primary objective of this study is to evaluate the first very tall tower
83 continuous eddy covariance flux measurement of CH_4 in a regional landscape. Further,
84 we compared the magnitude and variability of these observations to plot-scale wetland
85 and forest observations and model simulations. In late 2010, we instrumented a very
86 tall tower in northern Wisconsin USA to observe CH_4 turbulent fluxes at 122 m above
87 the ground and CH_4 concentration at 3 heights, sampling a spatially heterogeneous mix
88 of upland forest and lowland wetland systems (Fig. 1). The site has been measuring CO_2
89 and H_2O eddy fluxes and concentration at this height and the other two since 1996.
90 Since the pioneering studies using tunable diode laser spectroscopy-based eddy
91 covariance for CH_4 fluxes (Fowler *et al.*, 1995; Kim *et al.*, 1998; Shurpali and Verma,
92 1998; Suyker *et al.*, 1996), there have been a growing number of publications based on
93 short-term CH_4 flux observations (e.g., Friborg *et al.*, 2003; Hargreaves *et al.*, 2001;
94 Nicolini *et al.*, 2013). With the development of reliable, low-drift, closed and open path
95 methane analyzers (McDermitt *et al.*, 2011), it is now possible to maintain long time
96 series of CH_4 fluxes (e.g., Baldocchi *et al.*, 2012; Hatala *et al.*, 2012; Olson *et al.*, 2013;
97 Rinne *et al.*, 2007; Smeets *et al.*, 2009; Wille *et al.*, 2008). None of these measurements
98 have been made at the landscape scale (25-100 km^2) from a very tall tower, and only a
99 subset of these studies report simultaneously on CH_4, CO_2, and H_2O flux measurements.
100 The value of continuous observations at landscape scales is to directly observe to
101 what extent episodic and spatially heterogeneous emissions influence the net annual
102 budget of biospheric CH_4 fluxes. Only continuous observations, for example, can
103 regularly capture (or record) pulses of CH_4 (e.g., after a rainstorm or during ebullition

events) (Strack and Waddington, 2008) along with non-growing season fluxes, which may also be substantial (Pelletier *et al.*, 2007; Yu *et al.*, 2007).

We seek to understand the nature of regional or landscape-scale net ecosystem exchange of CH_4 (NEE CH_4). In theory, we would expect that if wetland CH_4 production (Reco_CH_4) dominates forest CH_4 consumption and wetland CH_4 oxidation, then the landscape CH_4 flux would be proportional to the wetland spatial extent and its mean flux as measured by chambers. Also, some ecosystem models simulate CH_4 production based on assuming a constant ratio of either ecosystem respiration (R_{eco}) to R_{eco} or NEE CO_2 to NEE CH_4 at annual timescales (e.g., Potter et al., 1997). To investigate these claims, we ask:

- What is the magnitude of NEE CH_4 in a mixed forest-wetland landscape and how does it compare to site-level chamber-based estimates?
- How predictive are environmental factors such as water table and temperature or other biogeochemical fluxes such as Reco_CO_2 or NEE CO_2 on daily to interannual variability of NEE CH_4?
- How well does a state-of-the-art ecosystem model simulate landscape NEE CH_4?

2. Methods

2.1 Site description

Methane flux and profile measurements were made at the WLEF very tall tower US-PFa Fluxnet site (Davis *et al.*, 2003) in Wisconsin, USA (45.945° N, 90.273° W). The surrounding landscape (Figure 1) is a representative mix of forested and open wetlands (28% in entire region (~50 km), 18% within 5 km of tower) with the remainder primarily composed of mixed deciduous and evergreen forests with most stands

ranging from 30 to 70 years old. Most of the landscape is within the Chequamegon-Nicolet National Forest and forests that are actively managed for multiple purposes, including recreation, wildlife habitat, and timber production. Wetlands in the region include both open fens and forested bogs and a smaller proportion of open-water bodies. Upland stands are generally characterized by mixed northern hardwood species (*Acer saccharum, Tilia americana, Fraxinus pennsylvanica, Betula papyrifera*); early- to mid-successional aspen-fir (*Populus tremuloides, Populus grandidentata, Abies balsamea*); and pine-spruce (*Pinus resinosa, Pinus banksiana, Picea glauca*). Lowlands are generally characterized by wetland shrub and sedge species in fens and along stream banks (*Alnus rugosa, Salix spp., Carex spp.*); deciduous hardwood species in retired and seasonal drainageways (*Fraxinus nigra, Ulmus rubra, Acer rubrum*); ericaceous shrubs and moss in open bogs (*Chamaedaphne calyculata, Ledum groenlandicum, Sphagnum spp.*); and wetland conifers in drier peatlands and bog edges (*Thuja occidentalis, Larix larcina, Picea mariana, Abies balsamea*).

The site has an interior continental climate with cold winters and warm summers (Table 1). Precipitation is greatest in the spring and fall, though there is regular and abundant winter snowfall. Over the two decades of flux tower CO_2 measurements, the site has varied from being a small source of CO_2 to a modest sink for CO_2 (Desai, 2014). Previous studies (Desai *et al*., 2008a) have indicated that the mean tower footprint samples a landscape that is representative of much of the Upper Midwest U.S. forested region, and the proportions of wetland and forest sampled are representative of the average wetland/forest coverage in the entire National Forest.

2.2 Very tall tower measurements

Flux measurements of CO_2, H_2O, heat, and momentum and associated tower profile meteorology and surface micrometeorology have been made continuously at the site since the middle of 1996 (Davis *et al.*, 2003). Flux measurements except for CH_4 have been made at three heights above ground, 30 m, 122 m, and 396 m. CO_2 and H_2O flux measurements at each level were made with a Licor, Inc. LI-6262 infrared gas analyzer and ATI Type K sonic anemometers (Table 1). Each level has a gas analyzer in a trailer at the tower base with large vacuum pumps drawing air to them. For the upper two levels, an additional gas analyzer was placed on tower at their respective heights to minimize data loss and account for flux loss for long tube lengths. Generally, fluxes between the on tower sensors and the long tube length sensors compared favorably, especially after high frequency spectral loss corrections were applied (Berger *et al.*, 2001). All flux instruments were sampled initially at 5 Hz, but switched to 10 Hz in 2006. In addition to the flux measurements, each level has measurements of temperature and humidity (Vaisala, Inc. HMP45C). Measurements of incoming above-canopy photosynthetically active radiation (PAR) were made at the base of the very tall tower. Precipitation and soil moisture were made at a nearby stand-scale flux tower (US-WCr) and compared and gap-filled with other micrometeorological stations within 30 km of the tower.

In the middle of 2010, we installed a cavity ring-down spectrometer (Picarro Inc., model 1301-f) for measurement of continuous CO_2 and CH_4 concentration at the 122 m level. This instrument is one of several new instruments with high sensitivity for continuous high-frequency CH_4 measurements that have arisen since the development of low-cost quantum cascade and infrared lasers (Kroon *et al.*, 2007), with limited sensor calibration drift (Hendriks *et al.*, 2008). The instrument was housed inside a

174 temperature-controlled trailer and sub-sampled air diverted from the 122 m level LI-
175 6262 analyzer. A second pump was applied to draw air into the Picarro cavity. The
176 Picarro analyzer maintains a constant pressure and temperature in the cavity and
177 directly reports mole fraction of the gas species. We did not attempt to sync the LI-6262
178 water vapor signal to estimate 10 Hz CH_4 dry air mixing ratio, but rather applied a
179 Webb-Pearson-Leuning (WPL, Webb *et al.*, 1980) correction as discussed below.
180 Storage flux was derived from profile measurements of CO_2 and CH_4 made on the
181 tower. CO_2 profile measurements were made with a Licor, Inc. LI-7000 analyzer
182 maintained by the National Oceanographic and Atmospheric Administration (NOAA)
183 Earth Systems Research Lab (ESRL) (Andrews *et al.*, 2014). These measurements have
184 been made since 1995 with a Licor 6251, which was replaced by the LI-7000 in May
185 2009. A separate set of intakes at the same heights as the flux tower levels provided air
186 to the analyzer, which performed 5-minute sequential sampling of each level. These air
187 samples were dried, flow controlled, and calibrated with zero and span gases multiple
188 times per day. In spring 2010, we installed a Los Gatos, Inc. LGR Fast Methane Analyzer,
189 drawing dried and conditioned air from the NOAA ESRL system and added standards
190 with known CH_4 concentration for calibration. Both profile measurements used in this
191 study were acquired from calibrated and interpolated time series of CO_2 and CH_4
192 concentrations from the three flux heights.
193 Flux and meteorology measurements were acquired with Campbell Scientific, Inc.
194 data loggers, except for the Picarro, which has its own internal storage system. To
195 maintain time alignment, all loggers and computers were synced to NIST UTC internet
196 time on an hourly basis. Flux data processing for CO_2 and H_2O fluxes was virtually
197 unchanged from Berger *et al.* (2001). The observed CO_2 concentrations were calibrated
198 against the NOAA ESRL on tower CO_2 observations within a 24-hour window, and

199 similarly water vapor was calibrated to water vapor mixing ratio obtained from on
200 tower Vaisala HMP45C sensors and surface barometric pressure measurements.
201 Picarro CO_2 and CH_4 observations had very small drift and have not shown any need for
202 calibration beyond factory calibration. A WPL correction for dilution by water vapor is
203 needed to obtain the dry air mole fraction of CO_2 and CH_4, using the approach of Hiller
204 *et al*. (2012). We opted not to apply the direct correction method of Baldocchi *et al*.
205 (2012) and Detto *et al*. (2011) as lining up H_2O observations from the LI-6262 to the
206 Picarro at 10 Hz was not easily possible, except for limited periods, where we did
207 compare the two approaches.
208 Sonic anemometer data were rotated to long-term (12-month) planar fits. Air
209 sampling lags were identified with maximal lagged covariance, and high-frequency
210 empirical spectral corrections were applied (Berger *et al*., 2001). Given the larger
211 eddies present at 122 m, we have previously showed that an hour-long averaging time
212 is more appropriate. (Berger *et al*., 2001).
213 One particular issue with our set up was drifting clocks between the Picarro and
214 the datalogger that stores the sonic data, even with regular time syncing. Further, the
215 Picarro's raw data are not stored at regular time intervals owing to data processing and
216 laser control sequence. We used a nearest neighbor approach for each time stamp,
217 essentially following the method of Eugster and Plüss (2010) to line up time stamps to
218 the sonic anemometer, with replication if needed. Lag corrections were applied after
219 this. Clock drift owing to malfunctioning computer clocks was obvious in the long-term
220 time series of lag times, requiring manual adjustment of the window of acceptable lag
221 times.
222 Additional quality control was applied, including range checks, spike detection,
223 and low turbulence filtering. We applied a 0.2 m/s u* filter for low turbulence at night.

For CO_2 and H_2O fluxes, where multiple heights and sensors were available, a preferred intake height algorithm (Davis *et al*., 2003) was applied to combine the independent flux observations, preferring higher levels in daytime and the lowest level at night during periods of negative heat flux, indicating decoupling of higher intake heights from the surface layer, as described in Davis *et al*. (2003).

While systematic biases are possible from assumptions made in data filtering, calibration, and flux algorithms, there is also the issue of random flux uncertainty. Given the sporadic nature of CH_4 emissions against a low background flux at most sites, turbulent flux uncertainty can be large relative to flux magnitude (Kroon *et al*., 2010). To estimate flux uncertainty for CH_4, we applied the method of Salesky *et al.* (2012). Flux uncertainty was derived from successive computation of eddy fluxes with longer averaging times, estimating the standard deviation of these sub-hour fluxes and extrapolating them to the hour to estimate flux uncertainty. Computationally, this calculation of fluxes at all averaging times up to one hour was done in Fourier spectrum to speed computation time. The method has been shown by Salesky *et al.* (2012) to be reliable and comparable to other methods based on random flux shuffling (Billesbach, 2011). For daily and cumulative errors, hourly errors were summed by squares after accounting for temporal autocorrelation up to a 24 hour lag.

For calculation of seasonal and annual fluxes, we also gap-filled the flux measurements of CO_2 and CH_4 and inferred Gross Primary Production (GPP) and Ecosystem Respiration (ER). CO_2 fluxes were gap-filled and partitioned by using the method described in Desai *et al*. (2005), based on a moving-window regression of quality controlled nighttime net ecosystem exchange of CO_2 (NEE CO_2) and a fit of daytime observations to incoming photosynthetically active radiation (PAR). This

method has compared favorably to other methods in common usage (Desai *et al*., 2008b).

There is currently no generally-accepted method for gap-filling for CH_4 fluxes. Our initial attempts at similar regression approaches as for NEE CO_2 at the hourly scale did not find strong relationships, similar to what has been reported by others (e.g., Dengel *et al*., 2013). Short gaps (<4 hours) at the hourly scale were filled with linear interpolation. However, at the daily scale, a stronger relationship with temperature allowed us to apply a second order polynomial fit between CH_4 daily flux and air temperature, accounting for random flux uncertainty as described above. While soil temperature would be possible for the fetch of a stand-level tower (10-30 m), there is no single estimate of regional soil temperature, and thus air temperature is the best metric of regional average ecosystem temperature. Further, we modeled random flux uncertainty as a linear function of mean flux to extrapolate random uncertainty of the gap-filled daily fluxes, to which we summed with the one-sigma uncertainty of the regression to estimate total random uncertainty. We also separately estimated gap-filling uncertainty by repeated calculation of annual sums of NEE CH_4 with differing regression coefficients based on their uncertainty.

Finally, flux footprints were estimated for each hour to estimate source contribution and potential footprint bias. We applied the empirical CBL model of Wang *et al*. (2006), which relies on similarity theory to derive mean Gaussian surface influence functions as a function of boundary layer characteristics such as convective velocity scale (w*), boundary layer depth (h), roughness height (z_0), and Monin-Obhukov length (z/L). These were used to confirm representative sampling of land cover in the tower climatological footprint as shown in Fig. 1

2.3 Plot-level observations

For comparison of regional fluxes from the tower to *in situ* CH_4 fluxes, we analyzed static chamber flux measurements made in four wetlands and three upland forests near the very tall tower (within 20 km, though not necessarily within the flux footprint). Static chamber measurements were made in the growing seasons (May-Sep) of 2005 and 2006 based on syringe sampling from closed, vented PVC chambers (25 cm diameter, 10 cm height). Chamber headspace samples (15 mL) were collected four times during a 30-minute period, with each sample transferred to an air-tight vial for transport to the laboratory. Vials were analyzed for CH_4 concentration by gas chromatography using a flame ionization detector (Hewlett Packard, 5890A) with calibrated standards (Scott Specialty, Inc.). Fluxes were calculated based on the increase in headspace concentration over time (Weishampel and Kolka, 2008). At each site, 3 plots containing 4 subplots each with 3 fixed, static chamber collars were sampled approximately monthly across the growing season (days of year 100 to 278). Mean soil temperature and volumetric soil water content were also measured in the plots at each flux sampling time point.

Wetland sites included an open, sphagnum-dominated bog (South Fork, SF; 45°55.37' N90°07.92' W)), a sedge-dominated riparian fen (Wilson Flowage, WF; 45°48.99' N, 90°10.29'W), an alder-dominated riparian wetland (Lost Creek, LC; 46°04.96' N, 89°58.72' W), and a cedar swamp (CS; 45°56.53' N 90°16.21' W). Forest sites included one mature deciduous forest, Willow Creek (WC; 45° 48.47' N, 90° 04.72' W), and two recent clear-cut (< 10 years at time of sampling) deciduous forests, Riley Creek (RC; 45°54.53' N, 90°07.27' W) young aspen and Thunder Creek (TC; 45°40.239' N 90°03.25' W). In this study, we were primarily interested in the mean and range of the wetland emissions and forest soil methane consumption over the entire growing season.

297 In addition, for comparison purposes, we also upscaled the chamber
298 measurements using flux footprint-weighted estimates of wetland and forest cover
299 multiplied respectively by mean and standard deviation of wetland and forest chamber
300 fluxes over all collars, all sites, and all growing season sampling dates (assuming 179
301 day growing season), assuming no methane exchange in winter or for other land cover
302 types. Intra and inter site variability across collars was propagated via Monte Carlo
303 sampling to estimate sensitivity of upscaling.

304 ## 2.4 Numerical modeling

305 The Dynamic Land Ecosystem Model (DLEM) is a comprehensive terrestrial
306 ecosystem model that couples carbon, nutrient and water cycles in terrestrial
307 ecosystems for estimating the hydrological and biogeochemical fluxes and pool sizes at
308 multiple scales from site to region/globe and with time step ranging from day to year.
309 Through carbon-nutrient-water coupling, DLEM is capable of simultaneously depicting
310 the biosphere-atmosphere exchange of CO_2, CH_4 and N_2O under multiple natural and
311 anthropogenic disturbances (Tian *et al*., 2010). The model can simulate regional
312 hydrology including evapotranspiration, runoff and soil moisture (Liu *et al.*, 2013). Here,
313 we ran the model in two modes over the study period: a cut-out of a previously
314 continental-scale regionally parameterized model and a single site-level model. The
315 regional model was cut-out from a spatial resolution of 5 by 5 arc-minutes (around 9.2 ×
316 9.2 km grid at the equator), using default land cover for the grid cell. The site model was
317 run with local estimates of wetland and forest cover. There is large difference in the
318 percent area of three major plant functional types between regional data and site data
319 (Table 2). The site model experiment was run with gap-filled tower observed
320 meteorology, whereas the regional model was run with large-scale gridded meteorology

(Climate Research Unit National Center for Environmental Prediction - CRUNCEP). We ran the model in site and regional modes to assess biases in modeling of regional CH_4 flux.

3. Results

3.1 Fidelity of very tall tower flux

Methane eddy covariance flux measurements in 2011 and 2012 were successfully made over 68% of the time (Table 3). An additional 13% of all available hours were filtered for low turbulence conditions ($u^* < 0.2$ m s^{-1}). Spectral loss from long tube lengths and lag times were nearly identical for NEE CO_2 and NEE CH_4 and similar to earlier results published in Berger *et al*. (2001). Flux observations sampled a footprint (Fig. 1) with an average fetch in any one direction of 1-4 km and sampled all wind sectors. The relatively self-similar pattern of wetlands and forests in the fetch allowed for a "homogenous" sampling of diverse upland and lowland ecosystems around the tower. However, given the lower amount of wetland in the immediate vicinity of the tower compared to the larger region, the 2011 footprint climatology showed an average wetland sampling of 17%, with forests at 70%, and other covers (grass, water, roads, shrubs) at 13%. Daytime and nighttime footprints were similar, except for slightly enhanced contribution of the ~100 m diameter grassy clearing surrounding the tower during the daytime.

Flux observations of methane had turbulent behavior quite similar to CO_2. WPL correction for water vapor dilution was found to be modestly important for NEE CH_4 from closed path analyzers (Fig. 2). WPL corrected NEE CH_4 was on average 1.2% larger than uncorrected. We also tested whether a WPL correction was similar to the direct

dry air mixing ratio flux calculation. Over a one month period, H_2O mixing ratio observations were synced in time and used to directly compute dry mole fraction CH_4 at 10 Hz. Our results showed strong correlation and low bias, but on average, the direct dry-air NEE CH_4 were 1.6% larger than WPL-corrected flux, or overall nearly 3% larger than uncorrected NEE CH_4 (Fig. 2).

Because methane fluxes at the site were small, random turbulent uncertainty could be a significant component. Our application of the Salesky *et al*. (2012) method revealed a baseline uncertainty (level of detection) of NEE CH_4 to be 0.13 nmol CH_4 m^{-2} s^{-1} at the hourly scale and 0.42 mg C-CH_4 m^{-2} day^{-1} at the daily scale. Over the two year study period, 2.2% of hours had a NEE CH_4 magnitude below that amount, though 15.2% of daily NEE CH_4 was below the daily threshold, primarily during the winter. Average uncertainty was 20% for hourly fluxes and 12% for daily fluxes (Fig. 3). However, at the hourly or daily scale, uncertainty only weakly scales with flux magnitude. These uncertainty estimates were propagated in estimates of total annual flux, as discussed below.

For very tall tower measurements, the contribution of below sensor height storage flux can be significant for all fluxes with strong surface sources or sinks, especially at night (Fig. S1). Storage flux magnitude contributed a median of 48% of the total NEE CH_4 magnitude around noon, but 75% of the nighttime NEE CH_4 at the hourly scale. Storage flux declines to zero as averaging timescale increases. Nonetheless, this flux cannot be neglected for hourly to daily NEE CH_4 observations from very tall towers, especially at night. For NEE CO_2 and NEE CH_4, storage flux is on the same order as eddy flux at night, though the largest magnitude contribution of storage flux occurs shortly after sunrise, when flushing of accumulated nighttime CO_2 or CH_4 near the surface leads to a strong negative storage flux, which quickly declines to zero by solar noon. However,

for CH_4, this peak occurs roughly 1-2 hours later than for CO_2, and the decline to zero is more gradual and also shifted by a similar amount. Further, in the morning during the growing season, flux and storage terms for NEE CO_2 are the same sign (negative), while for NEE CH_4, they are opposite signs (positive for eddy flux, negative for storage), leading to a possibly greater source of error for diurnal fluxes of NEE CH_4, especially if storage and eddy fluxes have differing source area contribution. For daily NEE, this effect is negligible as average daily storage flux for CH_4 is < 4% of daily NEE CH_4.

3.2 Comparison to plot-level chamber observation

Plot level chamber methane fluxes (Fig. 4a) reveal significant within and across site differences in collar-averaged daytime CH_4 fluxes across the four wetland (193 measurements) and three upland forest study sites (152 measurements) in the region. Tower observed daytime growing-season NEE CH_4 have efflux rates that bracket the static chamber observations, with most tower observations occurring in-between the largest and smallest wetland flux observations. Tower maximum efflux rates do not generally exceed those observed at the high CH_4 emission sedge site, where plant-mediated pathways and high proportion of labile carbon likely facilitated CH_4 flux. Chamber CH_4 exchange from wetland or upland forest sites had significantly different distributions than tower NEE CH_4 (Wilcox Rank-Sum U-Test $p<0.001$). The average daily efflux of CH_4 from all sampled wetlands was 5.08 +/- 15.3 nmol CH_4 m^{-2} s^{-1} and average forest soil uptake was -1.8 +/- 1.1 nmol CH_4 m^{-2} s^{-1}. Tower mean NEE CH4 averaged over the period corresponding to the earliest and latest sample dates (days of year 100-278) was 3.9 +/- 11.2 nmol CH_4 m^{-2} s^{-1}. Large negative values of NEE CH_4 observed by the tower were much larger than any observed at chamber sites. The highest magnitude of chamber CH_4 emissions was observed from the groundwater fed

393 sedge dominated wetland (WF), which promoted plant-mediated transport and was
394 wetter than the other sites.
395 While upscaling is of limited value given the amount of chamber data available, it
396 can provide some estimate of whether the chamber fluxes are representative of the
397 landscape flux. Mean chamber-based upscaled NEE CH_4 was 145 +/- 436 mg C-CH_4 m^{-2}
398 s^{-1} from wetlands and -214 +/- 131 mg C-CH_4 m^{-2} s^{-1} from forests. This amounts to a
399 total upscaled NEE CH_4 of -64 +/- 567 mg C-CH_4 m^{-2} s^{-1}, as the forest CH_4 sink essentially
400 cancels out wetland emissions. Tower observations show a net source of 785 +/- 75 mg
401 C-CH_4 m^{-2} s^{-1} observed by the tower. Wetland chamber emissions alone are less than
402 20% of the tower observed source. Caution is required as the chambers were sampled
403 in different years (2005-2006) from the tower (2011-2012). Summer mean
404 temperatures for chamber observations in 2005-2006 were 0.25 °C warmer and 2%
405 wetter on average compared to tower observations in 2011-2012. These findings
406 highlight the need to better delineate wetland type and area, peat depth, edge effects,
407 and decomposability for accurate upscaling.

408 ### 3.3 Seasonal and interannual patterns of carbon fluxes

409 Patterns of daily CH_4 (Fig. 5a), CO_2 (Fig. 5b) fluxes and inferred GPP (Fig. 5c) and
410 R_{eco} (Fig. 5d) at the site showed seasonal patterns typical of temperature-limited
411 temperate mixed forest regions. NEE of CO_2 and CH_4 were generally negatively
412 correlated at a monthly scale (Table 4). Peak uptake of NEE CO_2 was in early to mid-
413 summer, while NEE CH_4 showed higher daily variability and lacked a distinct early-mid
414 summer peak. Patterns of NEE for CO_2 and CH_4 were similar in both years, but 2012
415 featured both an earlier growing season start and a pronounced drought in the mid-
416 summer (Jul-Sep) (Fig. 6c). While drier in the growing season, the earlier green-up led

417 to higher GPP in 2012 for most of the growing season (Fig. 5c), and higher R_{eco} from
418 mid-summer onward. The period of high ecosystem respiration was not directly related
419 to any reduction of CH_4 emissions, a feature only apparent at the annual scale. Both
420 years had growing seasons (May-Sept) that were 10-28% drier and 0.4-0.8^{o}C warmer
421 than the long-term (1995-2013) average.
422 NEE CH_4 exhibited periods in both the winter and growing season of high
423 emissions relative to the average for the time period (Fig. 5a). These "bursts" were
424 primarily generated in the turbulent flux term, were more common and prominent for
425 CH_4 than CO_2, were skewed in the positive direction, and were not coincident with
426 excursions in NEE CO_2, nor were they consistently co-occurring with large pressure or
427 turbulence changes or any known fossil-fuel CH_4 sources. These high emission days in
428 summer also exhibited relatively high turbulent flux uncertainty and were more
429 pronounced in 2011 than 2012. NEE CH_4 hourly bursts that exceed two standard
430 deviations from a background seven-day average over the measurement period
431 occurred only 6% of the time, but they contributed nearly a quarter of the absolute flux,
432 which adds a further challenge to gap-filling, which in our current version cannot
433 capture these events. Unfortunately, during the anomalously warm early spring of 2012,
434 CH_4 flux observations were not available. Spectral analyses of the modes of variability
435 for gap-filled NEE CO_2 and NEE CH_4 from 2011-2012 show that the contribution of
436 timescale to NEE CH_4 is relatively similar to NEE CO_2, though NEE CH_4 scale has reduced
437 contribution of variation from the monthly (20-30 day) scale and greater contribution
438 at the seasonal (> 100 day) scale (Fig. 7b).
439 Overall, annual NEE CH_4 from the region is relatively small in magnitude, on
440 average 1.1% of the NEE CO_2 by mole or mass fraction (Table 3). Cumulative NEE CH_4
441 (Fig. 7a) in the two years averaged 785 +/- 75 mg C m^{-2} yr^{-1} while NEE of CO_2 was -157 g

C m^{-2} yr^{-1}. CH_4 fluxes were lower in 2012, though just outside the uncertainty bounds arising from both gap-filling and flux random uncertainty. In 2012, CH_4 fluxes appear to be suppressed in the early to mid-growing season in slightly warmer, but wetter conditions compared to the previous year, though the presence of gaps in part of this period complicates the analysis. The remaining part of the growing season has a similar pattern of net emissions as the prior year (Fig. 5).

The shifts in R_{eco} and CH_4 NEE in 2012 were likely related to the 1.3 °C higher annual air temperature in 2012 and lack of precipitation in late July through August in 2012 (Table 3). Warmer air temperatures in 2012 led to a very early growing season, and a quasi-stationary ridge of high pressure promoted longer periods of dry, warm conditions in summer 2012. While the reduction in precipitation is not particularly large, there was a significant change in timing of precipitation (Fig. 6c), depressing 2012 soil moisture through the late summer and fall (Fig. 6d).

Interannual variability of CH_4 flux between the two years is 32% of the mean flux, slightly larger than variability in GPP (29%) and R_{eco} (28%), but different than for NEE CO_2 fluxes over this time (54%), as the longer growing season (increased GPP) in 2012 more than offset the warmer, drier conditions in the same year (increased R_{eco}). The consequence of the longer growing season and warmer conditions was that GPP increased by 35%, while R_{eco} increased by 32% between 2011 and 2012, whereas annual CH_4 fluxes declined by 28%. Interannual variability in prior years for CO_2 NEE has been larger. The range of annual CO_2 fluxes measured from 1996-2012 exceeded 296 g C m^{-2} yr^{-1} (Desai, 2014), as the site has shifted from being a net source of CO_2 to a net sink in some years.

3.4 Growing season diurnal patterns

Diel patterns for methane are particularly unique showing an early to mid-morning negative peak in CH_4 fluxes in contrast to a late morning peak for NEE CO_2, and near noon peak for GPP, and afternoon peak for R_{eco} (Fig. 8), as the latter two follow patterns of PAR and air temperature. Methane reaches a minimum between 8-10 local time (LST), but the minima shifts earlier in 2012, and variability in diurnal pattern is large. While the relative change in hourly NEE was small between 2011 and 2012, there are distinguishable changes in R_{eco} and GPP which were large and compensating. For CH_4, a decrease in NEE CH_4 from 2011 to 2012 is seen in the average for all hours, but variability in this mean is large. There is, however, a decrease in variability around the mean in 2012 compared to 2011, perhaps reflecting the changes in areal coverage of inundated areas contributing episodic methane emissions, given lower soil moisture as a result of decreased late summer precipitation in 2012.

3.5 Environmental controls on regional methane flux

Variations in CO_2 NEE are typically well described by variations in PAR and temperature at the hourly scale (Desai, 2014), but these correlations were only apparent for CH_4 when averaged at daily to weekly time scales (Table 4). Correlation of NEE CH_4 to NEE CO_2 is significant and negative, but weaker in effect size than for PAR and T. Further, at monthly timescales, the correlation for NEE CH_4 is greatest for R_{eco} and GPP. Interestingly, this relationship with R_{eco} is positive, implying that greater R_{eco} is associated with greater emissions of CH_4 in the region. However, this relationship does not hold at the interannual scale, where increased R_{eco} in 2012 is accompanied by decreased NEE CH_4 (Table 3).

It is likely that the positive correlation of R_{eco} and NEE CH_4 at the shorter time scales primarily reflects the exponential nature of these processes with respect to temperature (Fig. 9). Scatterplots of NEE CH_4 versus temperature and GPP are only weakly correlated at the hourly scale, partly owing to the high uncertainty of NEE CH_4. For daily average NEE CH_4, a linear relationship to GPP and exponential relationship to temperature are more apparent. For the exponential relationship to temperature, daily NEE CH_4 is relatively insensitive for air temperature of 0-15 °C, followed by a large increase in emissions with higher temperature (Fig. 9d). Regionally, it appears at short timescales, that CH_4 production and its relationship to temperature dominates any increase in longer-timescale changes in CH_4 oxidation that would occur with the lower soil moisture that co-occurs with high temperature.

3.6 Comparison to ecosystem models

The DLEM model output of daily NEE CH_4 for the region (only available in 2011) and site (2011-2012) reveals similar seasonal patterns to the very tall tower observations, but several discrepancies exist (Fig. 10). First, the regional model, run with an estimate of land-cover based on a continental gridded map, generated CH_4 emissions significantly larger than observed NEE CH_4, likely owing to the larger estimation of wetland area fraction in the regional model (Table 2). It also resulted in CH_4 emissions earlier in the spring and later in the autumn compared to observations. The site level run, using local estimates of wetland extent and local meteorology, had seasonal magnitudes much more in line with the tower. The site model still overestimated CH_4 emissions in the autumn. Further, the site model showed very little interannual variability, while the observations clearly showed a mid to late summer suppression of CH_4 emissions in 2012, likely in response to the lack of precipitation in

512 this time period. Finally, both models tended to have relatively modest sub-weekly
513 variability in CH_4 emissions, while observations showed much larger day-to-day and
514 monthly variation.

515 4. Discussion

516 4.1 Uncertainty of regional CH_4 flux

517 Our analysis confirms that current generation closed path methane analyzers
518 can reliably measure CH_4 fluxes, even in regions of small flux magnitude, as long as high-
519 frequency spectral corrections were applied, confirming recent cross-comparison
520 studies (e.g., Iwata *et al*., 2014). WPL water vapor dilution corrections were more
521 important for CH_4 than CO_2 given the two orders of magnitude smaller concentration of
522 CH_4 than CO_2 in air. Still, even with long tube lengths, CH_4 fluxes could be measured
523 reasonably to ~20% accuracy at the hourly scale, similar to results shown in recently
524 published papers on methane eddy covariance (Detto *et al*., 2011; Smeets *et al*., 2009).
525 Both large positive and negative short-term CH_4 pulses appear to be real, but could arise
526 from either ecosystem processes or vertical flux transport.
527 A bigger challenge in quantifying net CH_4 ecosystem exchange appears to be
528 finding an adequate gap-filling strategy, as relationships of CH_4 flux at the hourly scale
529 to meteorological drivers have far greater variability than for CO_2. New approaches
530 using artificial neural networks have shown promise (Dengel *et al*., 2013; Hatala *et al*.,
531 2012), but a standard community approach to gap-filling has not been identified.
532 Chamber flux measurements are also subject to measurement bias and
533 uncertainty and also from sampling bias. Static chambers and soil gradient techniques
534 have known biases and require averaging over large space and time scales to best fit

535 models (Levy *et al*., 2012), complicating most former and more elaborate upscaling
536 attempts in other regions (Hendriks *et al*., 2010; Schrier-Uijl *et al*., 2010). Wetland
537 measurement is particularly difficult as the placement of the chamber and soil
538 compaction during the measurement process by fieldwork can influence the flux. While
539 a recent intercomparison study showed that seasonal variations and magnitudes of
540 chamber fluxes agree well to stand-level eddy covariance observations of NEE CH_4 (Yu
541 *et al*., 2013), upscaling these plot and stand level observations to the region is not
542 straightforward, as high spatial heterogeneity complicates sampling strategies. Further,
543 since production, consumption, and oxidation responses of CH_4 to climate are non-
544 linear, extrapolating flux sensitivity from spatial variations across sites does not
545 necessarily lead to the same conclusions about CH_4 drivers as temporal variation within
546 sites (Sabrekov *et al.*, 2014).
547 Finally, estimates of scaled fluxes are highly sensitive to estimate of wetland and
548 forest extent in the case of chambers and for temporal variation of these within the flux
549 footprint for towers. Our chamber estimates argue that the small forest CH_4 sink
550 overwhelms wetland CH_4 emission mainly because forests have a much larger spatial
551 extent. Additionally, drier conditions in 2005-2006 compared to 2011-2012 may have
552 decreased wetland CH_4 production. It could also be the case that higher CH_4 estimate
553 from the flux tower suggests that chambers did not adequately sample high sources of
554 wetland CH_4 emission or over-estimated the forest CH_4 sink. For example, upland-
555 wetland edges could be particularly dynamic sources of CH_4 production, but are rarely
556 sampled.
557 The purpose of our upscaling was not to build a defensible NEE CH_4 from
558 chambers, but to estimate how well plot-scale measurements can sample landscape CH_4
559 flux. Our approach was necessarily simplistic due to constraints of sampling design.

Other attempts at upscaling based on vegetation maps (e.g. Reeburgh et al. 1998) point to the importance of capturing landscape CH_4 hotspots, such as wetlands. Within site and across site variation in CH_4 exchange among fens and bogs is large (Baldocchi *et al.*, 2012), and attempts to find optimal and efficient sampling designs for upscaling are not at hand.

Our results call into question the reliability of extrapolation of CH_4 plot scale flux studies for estimating global natural CH_4 emissions, which is urgently needed given that recent studies have suggested, but not conclusively shown, increases in global wetland CH_4 emissions in the past decade (Spahni *et al.*, 2011).

4.2 Magnitude of regional CH_4 flux

Average annual CH_4 efflux was a relatively small 785 +/- 75 mg C-CH_4 m^{-2} yr^{-1}, compared to a mean CO_2 sink of -80 g C-CO_2 m^{-2} yr^{-1}. The two years showed a 30% shift in CH_4 flux from one year to the next that was detectable outside the bounds of our uncertainty analysis. Regional CH_4 fluxes by eddy covariance also bracketed those observed by chamber fluxes in prior years in wetlands within the tower landscape.

Our results are similar qualitatively to the early CH_4 emission work of Shurpali *et al*. (1998), which showed modest CH_4 emissions and lack of strong short-term coupling between CH_4 fluxes and GPP in a Minnesota bog. Overall, our regional observations are about an order of magnitude larger than recently published eddy covariance forest CH_4 flux estimates (Shoemaker *et al.*, 2014) and 1-2 orders of magnitude smaller than a range of CH_4 eddy flux studies in a variety of wetlands, including deltas (Baldocchi *et al.*, 2012), rice paddies (Hatala *et al.*, 2012), grazing fields (Herbst *et al.*, 2011), boreal fens (Long *et al.*, 2009; Rinne *et al.*, 2007), peatlands (Pelletier *et al.*, 2007), marshes (Chu *et al.*, 2014), and tundra (Sachs *et al.*, 2008; Tagesson *et al.*, 2012; Wille *et al.*, 2008).

584 Areas of significant CH_4 emission do occur in the region. For example, recent
585 eddy covariance estimates of NEE CH_4 in a Minnesota fen from 2009-2011 show
586 emissions of 11.8-24.9 g C- CH_4 m^{-2} yr^{-1}, a value that amounted to 23-39% of the NEE
587 CO_2 sink (Olson *et al*., 2013). Similarly, Pypker *et al*. (2013) finds a northern Michigan
588 poor fen with May-Sept emission of 13 g C-CH_4 m^{-2} yr^{-1} and Chu *et al.* (2014) show
589 freshwater marsh emissions of 49.7 g C-CH_4 m^{-2} yr^{-1} and cropland emissions of 2.3 g C-
590 CH_4 m^{-2} yr^{-1} in northern Ohio.
591 Another independent approach to regional NEE CH_4 is the tall tower modified
592 Bowen ratio technique based on assuming similarity in the flux-gradient relationship in
593 profiles of CO_2 and CH_4 concentration (Werner *et al*., 2003). This method, when applied
594 to the very tall tower site, showed average emissions of 2.7 g C-CH_4 m^{-2} yr^{-1} in 1998,
595 which is more than three times the estimate here (Fig. 4b), and with a longer NEE CH_4
596 emission season (Mar-Oct). However, those results were from 1998, a year that was
597 much warmer (average annual temperature of 7.8°C) than the 2011-2012 average
598 (5.4°C). Further, the similarity approach has known biases during periods of weak
599 vertical gradients of CH_4 or CO_2 and assumption of directly scaling of NEE CH_4 with NEE
600 CO_2, whose correlation is weak at the hourly and daily scale in our study (Table 4). The
601 authors concluded that this region emits 40% less CH_4 than other regions at the same
602 latitude.
603 Another regional carbon cycling upscaling study in the nearby Northern
604 Highland State Forest, based on the literature, found a range of 1 to 20 g C-CH_4 m^{-2} yr^{-1}
605 for CH_4 emission, roughly 1-2% of the estimated net carbon uptake in the region, but
606 nearly 10% of that for wetlands and 10% of that for lake evasion (Buffam *et al*., 2011).
607 This estimated range of CH_4 flux was also found to be similar to the amount of carbon
608 lost from the terrestrial landscape as DOC runoff. While Buffam *et al*. (2011) noted large

609 uncertainty on the CH_4 emission term, our regional observation results are consistent
610 with a value closer to the lower end of the range used.

611 ### 4.3 Drivers of CH_4 regional net exchange

612 We were able to discern shifts in annual CH_4 flux arising from shifts in growing
613 season length, air temperature, and late summer drought. The late summer 2012
614 drought was primarily a consequence of shifts in precipitation timing (earlier) instead
615 of total precipitation magnitude. The early start of the growing season, which likely
616 increased transpiration demand, along with the lack of rain in late summer of 2012
617 conceivably suppressed CH_4 production from wetlands in the tower footprint, while
618 simultaneously increasing upland forest soil CH_4 uptake, though no single driver can
619 adequately explain hourly to daily NEE CH_4.

620 Our results are generally consistent with the numerous site-level studies that
621 have attempted to correlate CH_4 observations to environmental parameters such as
622 water table depth, temperature, vegetation type, CO_2 fixation and respiration rates,
623 atmospheric O_3, and/or microbe/organic matter quality. A review paper by Jungkunst
624 and Fiedler (2007) noted that most studies point to water table and soil temperature as
625 strong controlling factors, and they further note that latitudinal trends suggest that
626 anaerobic and aerobic decomposition are both important in boreal regions.

627 While the modified Bowen ratio study of Werner *et al*. (2003) showed
628 precipitation explained a greater fraction of variance in regional NEE CH_4 than
629 temperature in 1997-1998, our results support temperature as the primary driver at
630 the monthly to seasonal timescale and precipitation, which may drive the availability of
631 substrate suitable for anaerobic decomposition, as the most likely explanation for
632 variation at the interannual scale. Enzyme kinetics of CH_4 production, primarily

633 controlled by temperature, seem to drive most of the daily to seasonal scale variability,
634 with an exponential dependence consistent with a recent report by Durocher *et al*.
635 (2014), Other studies have further confirmed the strong role of temperature for short-
636 term CH_4 dynamics (Blodau *et al*., 2007; Tagesson *et al*., 2012; Rinne *et al*., 2007).
637 Hydrology and long-term moisture status appear to be the key controls for
638 seasonal to annual variability (of NEE CH_4, R_{eco} and GPP), consistent with a recent
639 water-table manipulation study by Ballantyne *et al*. (2013). Thus, long-term changes in
640 water table are expected to have a strong impact on wetland CH_4 and CO_2 emission
641 ratios (Davidson and Janssens, 2006). Results at other sites concur that peatlands and
642 tundra systems are particularly sensitive to water availability within the active layer
643 (e.g., Hendriks *et al*., 2007; van Huissteden *et al*., 2005), and peatland drainage or
644 restoration by flooding strongly influences CH_4 production (Merbold *et al*., 2009;
645 Turetsky *et al*., 2008; Waddington and Day, 2007). Long-term declines in water table
646 may lead to soil subsidence, community change, and invasion of upland species (Strack
647 and Waddington, 2007; Sulman *et al*., 2013), significantly altering CH_4 production and
648 oxidation.
649 Our results do not support net ecosystem photosynthesis (NEE, NPP, or GPP) as
650 the primary controller on CH_4 net flux at the regional scale. The concept of a fixed ratio
651 of GPP, NPP or NEE to CH_4 production or NEE that has been argued based on field
652 measurement synthesis and process-based models (Potter *et al*., 1997; Walter and
653 Heimann, 2000; Whiting and Chanton, 1993) is not apparent in the short term. The
654 ratios of NEE CH_4 to NEE CO_2 observed here (~1%) at the annual timescale fall within
655 values measured in short term experiments (<1-3%; King and Reeburgh, 2002; King et
656 al., 2002; Megonigal et al., 1999). Whiting and Chanton (1993) call net ecosystem
657 production (equivalent to NEE CO_2) the "master variable" in controlling NEE CH_4,

658 suggesting that a fixed 3% of NEE CO_2 is emitted as NEE CH_4. Clearly, even if this holds
659 to be the case in general, variation around the value can be large and is timescale-
660 dependent.
661 King *et al*. (2002) report on input of new substrate from GPP as a source of CH_4
662 emission, arguing that increased productivity provides greater labile substrate and
663 increased transport. In contrast, greenhouse studies have shown that CH_4 emissions
664 related to plant type tended to decrease with increasing plant biomass (Kao-Kniffin *et*
665 *al*., 2010). While GPP does correlate with NEE CH_4 at our site, much of the correlation
666 appears to be a co-varying effect of temperature on both processes at the seasonal scale.
667 Short-term variations in GPP or NEE CO_2 do not correlate highly with NEE CH_4, as the
668 primary role of production is not to directly promote methanogenesis, but provide
669 substrate, while redox conditions provide conditions favorable for CH_4 production.
670 However, plants can serve as a conduit of CH_4, and thus GPP may be a proxy for plant-
671 mediated transport (King *et al*., 1998; Matthes *et al*., 2014). However, these results are
672 difficult to interpret regionally, as the primary GPP signal is coming from forests in the
673 flux footprint. Perhaps higher forest GPP implies greater export of carbon to the
674 watershed, providing greater substrate for methanogenesis, which would require
675 monitoring of aquatic and dissolved carbon.
676 Our results also showed a relatively high amount of short-time scale variation in
677 NEE CH_4, greater seasonal variation than for CO_2, and an unusual diurnal pattern to CH_4
678 flux, with minimum fluxes in early to mid-morning. Several studies have argued that
679 atmospheric pressure changes (Sachs *et al*., 2008) or shear turbulence (Wille *et al*.,
680 2008) could drive episodic CH_4 emissions, and perhaps a venting effect (for the diurnal
681 cycle) and synoptic pressure changes (for the weekly-monthly variation) are leading to
682 the variation we observed. For example, storage fluxes of CH_4 act in the opposite

683 direction (negative) to turbulent flux (positive) during the day. It is the strong negative
684 storage fluxes associated with atmospheric venting that drive the minima.
685 Mastepanov *et al*. (2008) observed CH_4 bursts before soil freezing in a tundra
686 ecosystem. While our results also show a variety of emission spikes in winter and
687 summer, we have yet to find any particularly strong correlation to barometric pressure,
688 changes in atmospheric pressure, friction velocity magnitude (both above and below
689 the filtering threshold), or other measures of processes that could lead to "pumping" of
690 CH_4 from the soil and snow surface. Initial experimental tests involving melting snow
691 and changing suction pressure with a static chamber did not reveal any significant
692 variation in CH_4 fluxes. Fossil fuel combustion could be a source for CH_4, but the timing
693 of the bursts were not consistent with possible generator or traffic sources, which are
694 quite limited in the flux footprint.
695 Despite the predominance of upland forest in the flux footprint, the site still is a
696 net emitter of CH_4 in both years. Upland plants have not been shown to emit significant
697 quantities of CH_4 in the field (Kirschbaum and Walcroft *et al*., 2008). Generally, upland
698 soils promote methanotrophs and thus dry soils tend to consume CH_4 (Ullah and Moore,
699 2011). This rate is controlled primarily by diffusion processes in the soil (Ridgwell *et al*.,
700 1999). A recent synthesis of micrometeorological CH_4 emission estimates in forests
701 generally shows net CH_4 sources with an interquartile range of 1.33-5.45 nmol CH_4 m^{-2}
702 s^{-1} (Nicolini *et al.*, 2013). Another review of 120 papers on soil CH_4 consumption found
703 no universal predictive ability of soil consumption by environmental drivers, but
704 showed that coarser soils had the largest CH_4 uptake in temperate forests, with a mean
705 uptake in temperate forests of 428 +/- 2360 mg C m^{-2} yr^{-1} (Dutaur and Verchot, 2007).
706 This reported uptake is larger than the average observed in our plot-level chamber
707 measurements in upland forests.

Our study site did include a few lakes in the landscape, and recent studies have argued that lakes and rivers may be large sources of CH_4 (Bastviken *et al.*, 2011; Buffam *et al.*, 2011; Grossart *et al.*, 2011; Juutinen *et al.*, 2009). Some evidence from chambers also suggests particularly large CH_4 flux variability at wetland-upland edges (unpublished data). Finally, winter emissions have generally been undersampled in most studies (Merbold *et al.*, 2013), given logistical difficulty in measurement and assumption of small CH_4 fluxes. Our results also support limited CH_4 fluxes during periods of frozen soil and inactive vegetation. However, fluxes outside the growing season (May-Sept) still contributed 17% of the net annual flux, averaged over the two years, and thus cannot be neglected.

4.4 Recommendations for simulations

Demand for quantification of regional CH_4 balances is increasing (Luyssaert *et al.*, 2012), and models are ultimately required to move from diagnosis to prediction. While several wetland and CH_4 models exist (Cao *et al.*, 1996; Melton *et al.* 2013; Petrescu *et al.*, 2008; Potter *et al.*, 1997; Sonnentag *et al.*, 2008; Walter *et al.*, 2001; Zhang *et al.*, 2002; Zhuang *et al.*, 2004), many only weakly constrain hydrology, and only a few also include upland CH_4 biogeochemistry. Walter *et al.* (2001) review the most common approach, based on temperature, net primary production, substrate availability, and water table depth and show the importance of hydrologic drivers for latitudinal variation in CH_4 efflux.

Our analysis of the commonly used DLEM model results revealed a general agreement between model and very tall tower observations on seasonal pattern, but lack of correspondence at shorter or longer timescales. Further, the regional model significantly overestimated CH_4 emissions primarily due to differences in wetland

732 extent in the regional (based on a cut-out of a continental model of greenhouse gas
733 fluxes) versus site simulation (based on local meteorology and land cover), a common
734 source of uncertainty for regional to global modeling of NEE CH_4 (Melton *et al.*, 2013).
735 Most models tend to show a strong sensitivity to water table (Petrescu *et al.*, 2007),
736 wetland extent (Ringeval *et al.*, 2010), and vegetation decomposition rate (van
737 Huissteden *et al.*, 2009). Over North America, DLEM shows enhanced CH_4 emissions
738 from increased climate variability, nitrogen deposition, and atmospheric CO_2, with
739 climate variability dominating interannual variability (Tian *et al.*, 2010; Xu *et al.*, 2010).
740 Simple models that rely on a fixed CO_2 uptake to CH_4 emission ratio for a base amount
741 and exponential temperature functions to capture seasonal or short-term variability
742 (Potter *et al.*, 2006), are likely to neglect the importance of variations in water table
743 which can cause a site to shift between CH_4 source and CH_4 sink. Similar to the results
744 here, other models have generally been unsuccessful at capturing short-term variability
745 in CH_4 emissions (Petrescu *et al.*, 2007; Zhang *et al.*, 2012).

746 Wetland extent and methane emission datasets both lead to wide variation in
747 modeled (Melton *et al.*, 2013) and extrapolated (Petrescu *et al.*, 2010) estimates.
748 Further, scaling methane emissions as a function of GPP or NEE, as some models do, is
749 not universal. While some sites show as much as 20% of CO_2 uptake returned as
750 methane emissions on a per mole basis (Rinne *et al.*, 2007), the regional evaluation here
751 showed only a fraction of a percent.

752 5. Conclusion

753 Our results confirmed the suitability of tall towers for observation of regional
754 CH_4 fluxes. While mixed forest dominates the landscape and the net CO_2 exchange
755 budget, wetlands dominate the CH_4 emission budget. However, uncertainty on our very

tall tower flux measurement, owing to random uncertainty, lack of well-established gap filling protocols, and flux footprint variability all need better quantification in future studies to better constrain the components of the regional CH_4 budget.

The net fluxes over two years showed modest CH_4 emissions in the region, representing less than 1% of NEE CO_2 in a productive mixed forest-wetland landscape. While individual fens or bogs can have large emission rates, as seen in some of our chamber flux observations, the region as a whole may be a minor contributor. We found that the landscape-scale CH_4 fluxes positively correlate with temperature at diurnal to monthly timescales, similar to ecosystem respiration. However, from one year to the next, ecosystem respiration and net CH_4 flux responded in opposite directions, reflecting the shifts in aerobic to anaerobic respiration that occur in wetlands with changes in moisture availability, the availability of organic substrates for decomposition, and the presence of living plants (e.g., sedge species) that can facilitate the exchange of gases between subsoil environments and the atmosphere.

Simple models that scale CH_4 emissions with R_{eco} or NEE of CO_2 are thus both spatial- and temporal-scale dependent. Interestingly, our results also showed higher CH_4 fluxes from the tower than simple upscaling based on chambers but lower than flux tower studies in nearby fens, confirming the relatively high spatial variability of CH_4 fluxes in the landscape. These results are contrary to a general assumption that chambers and plot-level studies always overestimate CH_4 emissions due to their typical placement in ecosystems with high CH_4 emission.

The regional flux time series was able to reveal limitations in modeling of short-term and interannual variability in CH_4 emissions by a dynamic ecosystem model. While temperature and moisture appear to be the strongest controls of CH_4 flux in the region, they have a clear timescale dependence. Our results suggest that models built on (1)

temperature for short-term methane emission rate, (2) water table or moisture availability for long-term base emissions amount (or interannual variability), and (3) an estimate of wetland extent are most likely to successfully simulate regional methane fluxes. However, similar to other studies, we find models are unable to simulate short-term (sub-daily) variation in CH_4 emissions (Melton *et al.*, 2013). Future work on decomposing the regional fluxes by land cover will further aid in developing appropriate metrics for evaluation of regional-scale simulations of CH_4 cycling.

While wetlands and other natural sources of CH_4 are only 15-30% of the global CH_4 budget, they are the largest source of variability and a major source of uncertainty for atmospheric chemistry, air quality, and climate models (Arneth *et al.*, 2010). The vast majority of observational studies of CH_4 emissions are made at the scale of a plot or individual ecosystem. Regional scale studies, like the one conducted here, can provide estimates of CH_4 flux at a scale relevant to model evaluation.

Acknowledgments

This work was supported by National Science Foundation (NSF) biology directorate grants DEB-0845166 and DBI-1062204. We also acknowledge the contributions of R. Strand and J. Ayers at State of Wisconsin Educational Communications Board, K. Davis at The Pennsylvania State University, and P. Bolstad at the University of Minnesota. Static chamber measurements were supported by the USDA Forest Service Northern Global Change program. Jonathan Kofler and Jonathan Williams were funded by NOAA to provide site and CO_2 and CH_4 profile instrument support. This project contributes to the North American Carbon Program. Any use of trade, firm, or product names is for descriptive purposes only and does not imply endorsement by the U.S. Government.

Works Cited

Andrews, A.E., J.D. Kofler, M.E. Trudeau, J. C. Williams, D.H. Neff, *et al.*, 2014. CO_2, CO, and CH_4 measurements from tall towers in the NOAA Earth System Research Laboratory's Global Greenhouse Gas Reference Network: instrumentation, uncertainty analysis, and recommendations for future high-accuracy greenhouse gas monitoring efforts. *Atmos. Meas. Tech.*, 7:647-687, doi:10.5194/amt-7-647-2014.

Arneth A., S. Sitch, K. Butterbach-Bahl, A. Bondeau, N. de Noblet-Ducoudré, P. Foster, N. Gedney, I.C. Prentice, M. Sanderson, K. Thonicke, R. Wania, and S. Zaehle, 2010. From biota to chemistry and climate: Towards a comprehensive description of trace gas exchange between the biosphere and atmosphere. *Biogeosciences,* 7:121-149.

Baldocchi, D., M. Detto, O. Sonnentag, J. Verfaillie, Y. A. Teh, W. Silver, and N. M. Kelly, 2012. The challenges of measuring methane fluxes and concentrations over a peatland pasture. *Agricultural and Forest Meteorology*, *153*:177–187, doi:10.1016/j.agrformet.2011.04.013.

Ballantyne, D. M., J. A. Hribljan, T. G. Pypker, and R. A. Chimner, 2013. Long-term water table manipulations alter peatland gaseous carbon fluxes in Northern Michigan. *Wetlands Ecol Manage*, *22*(1):35–47, doi:10.1007/s11273-013-9320-8.

Bastviken, D., L. J. Tranvik, J. A. Downing, P. M. Crill, and A. Enrich-Prast, 2011. Freshwater Methane Emissions Offset the Continental Carbon Sink. *Science*, *331*(6013):50–50, doi:10.1126/science.1196808.

Bergamaschi, P., C. Frankenberg, J.F. Meirink, M. Krol, F. Dentener, T. Wagner, U. Platt, J.O. Kaplan, S. Körner, M. Heimann, E.J. Dlugokencky, and A. Goede, 2007. Satellite chartography of atmospheric methane from SCIAMACHY onboard ENVISAT: (II) Evaluation based on inverse model simulations. *J. Geophys. Res.*, 112:D02304, doi:10.1029/2006JD007268.

Bergamaschi, P. et al., 2010. Inverse modeling of European CH_4 emissions 2001–2006, *J. Geophys Res*, *115*(D22), doi:10.1029/2010JD014180.

Berger, B.W., K.J. Davis, C. Yi, P.S. Bakwin, and C.L. Zhao, 2001. Long-term carbon dioxide fluxes from a very tall tower in a northern forest: Flux measurement methodology. *J. Atmos. Ocean. Tech.*, 18(4):529-542.

Billesbach, D. P., 2011. Estimating uncertainties in individual eddy covariance flux measurements: A comparison of methods and a proposed new method. *Agricultural and Forest Meteorology*, *151*(3):394–405, doi:10.1016/j.agrformet.2010.12.001.

Blodau, C., N. Roulet, T. Heitmann, H. Stewart, J. Beer, P. LaFleur, and T.R. Moore, 2007. Belowground carbon turnover in a temperate ombrotrophic bog. *Global Biogeochem. Cycles*, 21:GB1021, doi:10.1029/2005GB002659.

Bloom, A. A., P. I. Palmer, A. Fraser, D. S. Reay, and C. Frankenberg, 2010. Large-Scale controls of methanogenesis inferred from methane and gravity spaceborne data. *Science*, *327*(5963):322–325, doi:10.1126/science.1175176.

Bousquet, P., P. Ciais, J.B. Miller, E.J. Dlugokencky, D.A. Hauglustaine, C. Prigent, G.R. Van der Werf, P. Peylin, E.-G. Brunke, C. Carouge, R.L. Langenfelds, J. Lathiere, F. Papa, M. Ramonet, M. Schmidt, L.P. Steele, S.C. Tyler, and J. White, 2006. Contribution of anthropogenic and natural sources to atmospheric methane variability. *Nature*, 443(28):429-443.

852 Buffam, I., M.G. Turner, A.R. Desai, P. Hanson, J. Rusak, N.R. Lottig, E.H. Stanley, and S.R.
853 Carpenter, 2011. Integrating aquatic and terrestrial components to construct a
854 complete carbon budget for a north temperate lake district. *Global Change*
855 *Biology*, 17(2):1193-1211, doi:10.1111/j.1365-2486.2010.02313.x.
856 Cao, M., S. Marshall, and K. Gregson. 1996. Global carbon exchange and methane
857 emissions from natural wetlands: Application of a process-based model. *J.*
858 *Geophys. Res.*, D101:14399–14414.
859 Chen, Y.-H. and R.G. Prinn, 2006. Estimation of atmospheric methane emissions between
860 1996 and 2001 using a three-dimensional global chemical transport model. *J.*
861 *Geophys. Res.*, 111:D10307, doi:10.1029/2005JD006058.
862 Chu, H., J. Chen, J. F. Gottgens, Z. Ouyang, R. John, K. Czajkowski, and R. Becker, 2014. Net
863 ecosystem methane and carbon dioxide exchanges in a Lake Erie coastal marsh
864 and a nearby cropland. *J. Geophys. Res. Biogeosci.,* 119,
865 doi:10.1002/2013JG002520.
866 Collins, W. D. *et al.,* 2006. Radiative forcing by well-mixed greenhouse gases: Estimates
867 from climate models in the Intergovernmental Panel on Climate Change (IPCC)
868 Fourth Assessment Report (AR4). *J. Geophys Res*, *111*:D14,
869 doi:10.1029/2005JD006713.
870 Crill, P., K. Bartlett, and N. Roulet, 1993. Methane flux from boreal peatlands. *Suo*,
871 43:173-182.
872 Davidson, E.A. and I.A. Janssens, Temperature sensitivity of soil carbon decomposition
873 and feedbacks to climate. *Nature*, 440:165-173, doi::10.1038/nature04514.
874 Davis, K.J., P.S. Bakwin, C. Yi, B.W. Berger, C. Zhao, R.M. Teclaw, and J.G. Isebrands. 2003.
875 The annual cycles of CO_2 and H_2O exchange over a northern mixed forest as
876 observed from a very tall tower. *Global Change Biology*, 9(9):1278-1293.
877 Dengel, S., D. Zona, T. Sachs, M. Aurela, M. Jammet, F. J. W. Parmentier, W. Oechel, and T.
878 Vesala, 2013. Testing the applicability of neural networks as a gap-filling method
879 using CH_4 flux data from high latitude wetlands. *Biogeosciences*, *10*(12):8185–
880 8200, doi:10.5194/bg-10-8185-2013.
881 Desai, A.R., Bolstad, P.V., Cook, B.D., Davis, K.J., and Carey, E.V. 2005. Comparing net
882 ecosystem exchange of carbon dioxide between an old-growth and mature forest
883 in the upper midwest, USA. *Agriculture and Forest Meteorology*, 128:33-55.
884 Desai, A.R., A.N. Noormets, P.V. Bolstad, J. Chen, B.D. Cook, B.D., K.J. Davis, K.J., E.S.
885 Euskirchen, C.M. Gough, J.G. Martin, D.M. Ricciuto, H.P. Schmid, J.W. Tang, and W.
886 Wang, 2008a. Influence of vegetation and seasonal forcing on carbon dioxide
887 fluxes across the Upper Midwest, USA: Implications for regional scaling.
888 *Agricultural and Forest Meteorology*, 148(2):288-
889 308, doi:10.1016/j.agrformet.2007.08.001
890 Desai, A.R., A.D. Richardson, A.M. Moffat, J. Kattge, D.Y. Hollinger, A. Barr, E. Falge, A.
891 Noormets, D. Papale, M. Reichstein, and V.J. Stauch, 2008b. Cross site evaluation
892 of eddy covariance GPP and RE decomposition techniques. *Agricultural and*
893 *Forest Meteorology*, 148(6-7): 821-838, doi:10.1016/j.agrformet.2007.11.012.
894 Desai, A.R., 2014. Influence and predictive capacity of climate anomalies on daily to
895 decadal extremes in canopy photosynthesis. *Photosynthesis Research*, 119, 31-
896 47,doi:10.1007/s11120-013-9925-z.
897 Detto, M., J. Verfaillie, F. Anderson, L. Xu, and D. Baldocchi, 2011. Comparing laser-based
898 open- and closed-path gas analyzers to measure methane fluxes using the eddy
899 covariance method. *Agricultural and Forest Meteorology*, *151*(10):1312–1324,
900 doi:10.1016/j.agrformet.2011.05.014.

Dlugokencky, E. J. *et al.,* 2009. Observational constraints on recent increases in the atmospheric CH_4 burden. *Geophys. Res. Lett*, *36*(18):1–5, doi:10.1029/2009GL039780.

Yvon-Durocher, G., A. P. Allen, D. Bastviken, R. Conrad, C. Gudasz, A. St-Pierre, N. Thanh-Duc, and P. A. del Giorgio, 2014. Methane fluxes show consistent temperature dependence across microbial to ecosystem scales. *Nature*, 507:488-491, doi:10.1038/nature13164.

Dutaur, L., and L. Verchot, 2007. A global inventory of the soil CH_4 sink. *Global Biogeochem. Cycles*, 21:GB4013, doi:10.1029/2006GB002734.

Eugster, W., and P. Plüss, 2010. A fault-tolerant eddy covariance system for measuring CH_4 fluxes. *Agricultural and Forest Meteorology*, *150*(6):841–851, doi:10.1016/j.agrformet.2009.12.008.

Fowler, D., K.J. Hargreaves, U. Sibka, R. Milne, M.S. Zahinser, J.B. Monrieff, I.J. Beverland, M.W. Gallagher, P. Ineson, J. Garland, and C. Johnson, 1995. Measurements of CH_4 and N_2O fluxes at the landscape scape using micrometeorological methods. *Philosophical Transactions: Physical Sciences and Engineerin*g, 351(1696) 339-356.

Friborg, T., T. R. Christensen, B. U. Hansen, C. Nordstrom, and H. Sogaard, 2000. Trace gas exchange in a high arctic valley. 2. Landscape CH_4 fluxes measured and modelled using eddy correlation data. *Global Biogeochem. Cycles*, 14:715-724.

Friborg, T., H. Soegaard, T. R. Christensen, C. R. Lloyd, and N. S. Panikov, 2003. Siberian wetlands: Where a sink is a source. *Geophys. Res. Lett.*, 30(21):2129, doi:2003GL017797.

Grossart, H.-P., K. Frindte, C. Dziallas, W. Eckert, and K. W. Tang, 2011. Microbial methane production in oxygenated water column of an oligotrophic lake. *Proceedings of the National Academy of Sciences*, *108*(49):19657–19661, doi:10.1073/pnas.1110716108.

Hargreaves, K.J., D Fowler, C.E.R. Pitcairn, and M. Aurela, 2001. Annual methane emission from Finnish mires estimated from eddy covariance campaign measurements. *Theoretical and Applied Climatology*, 70:203-213.

Hatala, J. A., M. Detto, O. Sonnentag, S. J. Deverel, J. Verfaillie, and D. D. Baldocchi, 2012. Greenhouse gas (CO_2, CH_4, H_2O) fluxes from drained and flooded agricultural peatlands in the Sacramento-San Joaquin Delta. *Agriculture, Ecosystems & Environment*, *150*:1–18, doi:10.1016/j.agee.2012.01.009.

Hendriks, D. M. D., J. van Huissteden, A.J. Dolman, and M.K. van der Molen, 2007. The full greenhouse gas balance of an abandoned peat meadow. *Biogeosciences*, 4:411-424, doi:10.5194/bg-4-411-2007.

Hendriks, D.M.D., A. J. Dolman, M. K. van der Molen, and J. van Huissteden, 2008. A compact and stable eddy covariance set-up for methane measurements using off-axis integrated cavity output spectroscopy. *Atmos. Chem. Phys.,* 8:431-443, doi:10.5194/acp-8-431-2008.

Hendriks, D. M. D., J. V. Huissteden, and A. J. Dolman, 2010. Multi-technique assessment of spatial and temporal variability of methane fluxes in a peat meadow. *Agricultural and Forest Meteorology*, *150*(6):757–774, doi:10.1016/j.agrformet.2009.06.017.

Herbst, M., T. Friborg, R. Ringgaard, and H. Soegaard, 2011. Interpreting the variations in atmospheric methane fluxes observed above a restored wetland. *Agricultural and Forest Meteorology*, *151*(7):841–853, doi:10.1016/j.agrformet.2011.02.002.

Hiller, R. V., C. Zellweger, A. Knohl, and W. Eugster, 2012. Flux correction for closed-path laser spectrometers without internal water vapor measurements. *Atmos. Meas. Tech. Discuss.*, *5*(1), 351–384, doi:10.5194/amtd-5-351-2012.

Iwata, H., Y. Kosugi, K. Ono, M. Mano, A. Sakabe, A. Miyata, and K. Takahashi, 2014. Cross-validation of open-path and closed-path eddy-covariance techniques for observing methane fluxes. *Boundary-Layer Meteorol*, *151*(1):95–118, doi:10.1007/s10546-013-9890-2.

Jungkunst, H.F. and S. Fiedler, 2007. Latitudinal differentiated water table control of carbon dioxide, methane and nitrous oxide fluxes from hydromorphic soils: feedbacks to climate change. *Global Change Biology*, 13:2668–2683, doi: 10.1111/j.1365-2486.2007.01459.x.

Juutinen, S., M. Rantakari, P. Kortelainen, J.T. Huttunen, T. Larmola, J. Alm, J. Silvola, and P.J. Martikainen, 2009. Methane dynamics in different boreal lake types. *Biogeosciences*, 6:209-223, doi:10.5194/bg-6-209-2009.

Kao-Kniffin, J., D. S. Freyre, and T. C. Balser, 2010. Methane dynamics across wetland plant species. *Aquatic Botany*, 93:107–113, doi:10.1016/j.aquabot.2010.03.009.

Kim, J., S.B. Verma, and D.P. Billesbach, 1998. Seasonal variation in methane emission from a temperate Phragmites-dominated marsh: effect of growth stage and plant mediated transport. *Global Change Biol.,* 5:433–440.

King, J. Y., and W. S. Reeburgh, A pulse-labeling experiment to determine the contribution of recent plant photosynthates to net methane emission in arctic wet sedge tundra, *Soil Biol. Biochem.*, 34, 173–180, 2002

King J. Y., Reeburgh W. S., and Regli S. K., 1998. Methane emission and tranport by sedges in Alaska: results of a vegetation removal experiment. J Geophys. Res. 102, 29083 – 29092.

King, J.Y., W.S. Reeburgh, K.K. Thieler, G.W. Kling, W.M. Loya, L.C. Johnson, and K.J. Nadelhoffer, 2002. Pulse-labeling studies of carbon cycling in Arctic tundra ecosystems: The contribution of photosynthates to methane emission. *Global Biogeochem. Cycles*, 16(4):1062, doi: 10.1029/2001GB001456.

Kirschbaum, M. U. F. and A. Walcroft, A., 2008. No detectable aerobic methane efflux from plant material, nor from adsorption/desorption processes. *Biogeosciences*, 5:1551-1558, doi:10.5194/bg-5-1551-2008.

Kroon, P., A. Hensen, H. Jonker, M. Zahniser, W. Van't Veen, and A. Vermeulen (2007), Suitability of quantum cascade laser spectroscopy for CH_4 and N_2O eddy covariance flux measurements, *Biogeosciences*, *4*:715-728, doi:10.5194/bg-4-715-2007.

Kroon, P.S., A. Hensen, H.J.J. Jonker, H.G. Ouwersloot, A.T. Vermeulen, and F.C. Bosveld (2010), Uncertainties in eddy covariance flux measurements assessed from CH_4 and N2O observations, *Agric. Forest Meteorol.*, 150(6):806-816, doi:10.1016/j.agrformet.2009.08.008

Levy, P. E. et al., 2012. Methane emissions from soils: synthesis and analysis of a large UK data set. *Global Change Biol*, *18*(5):1657–1669, doi:10.1111/j.1365-2486.2011.02616.x.

Liu, M., H. Tian, Q. Yang, J. Yang, X. Song, S. E. Lohrenz, and W.-J. Cai, 2013. Long-term trends in evapotranspiration and runoff over the drainage basins of the Gulf of Mexico during 1901–2008. *Water Resour. Res.,* 49:1988–2012, doi:10.1002/wrcr.20180.

Long, K. D., L. B. Flanahan, and T. Cai, 2009. Diurnal and seasonal variation in methane emissions in a northern Canadian peatland measured by eddy covariance. *Global Change Biol*, 16:2420-2435, doi:10.1111/j.1365-2486.2009.02083.x.

Luyssaert, S. et al., 2012. The European land and inland water CO_2, CO, CH_4 and N_2O balance between 2001 and 2005. *Biogeosciences*, *9*(8):3357–3380, doi:10.5194/bg-9-3357-2012.

Mastepanov, M., C. Sigsgaard, E. J. Dlugokencky, S. Houweling, L. Ström, M. P. Tamstorf, and T. R. Christensen, 2008. Large tundra methane burst during onset of freezing. *Nature*, *456*(7222):628–630, doi:10.1038/nature07464.

Matthes, J. H., C. Sturtevant, J. Verfaillie, S. Knox, and D. Baldocchi, 2014. Parsing the variability in CH_4 flux at a spatially heterogeneous wetland: Integrating multiple eddy covariance towers with high-resolution flux footprint analysis. *J. Geophys. Res. Biogeosci.*, 119:1322–1339, doi:10.1002/2014JG002642.

Matthews, E., and I. Fung, 1987. Methane emissions from natural wetlands: Global distribution, area, and environmental characteristics of sources. *Global Biogeochem. Cycles*, 1:61-86, doi:10.1029/GB001i001p00061.

McDermitt D., G. Burba, L. Xu, T. Anderson, A. Komissarov, B. Riensche, J. Schedlbauer, G. Starr, D. Zona, W. Oechel, S. Oberbauer, and S. Hastings, 2011. A new low-power, open-path instrument for measuring methane flux by eddy covariance. *Appl Phys B* 102:391–405.

Megonigal, J. P., S. C. Whalen, D. T. Tissue, B. D. Bovard, D. B. Albert, and A. S. Allen, A plant-soil-atmosphere microcosm for tracing radio- carbon from photosynthesis through methanogenesis, *Soil Sci. Soc. Am. J.*, 63, 665–671, 1999

Melton, J.R., R. Wania, E.L. Hodson, B. Poulter, B. Ringeval, et al., 2013. Present state of global wetland extent and wetland methane modelling: conclusions from a model inter-comparison project (WETCHIMP). *Biogeosciences*, 10, 753-788, doi:10.5194/bg-10-753-2013.

Merbold, L., W. L. Kutsch, C. Corradi, O. Kolle, C. Rebmann, P. C. Stoy, S. A. Zimov, and E.-D. Schulze, 2009. Artificial drainage and associated carbon fluxes (CO_2/CH_4) in a tundra ecosystem. *Global Change Biol*, *15*(11):2599–2614, doi:10.1111/j.1365-2486.2009.01962.x.

Merbold, L., C. Steinlin, and F. Hagedorn, F., 2013. Winter greenhouse gas fluxes (CO_2, CH_4 and N_2O) from a subalpine grassland. *Biogeosciences*, 10:3185-3203, doi:10.5194/bg-10-3185-2013.

Mikaloff Fletcher, S. E., P. P. Tans, L. M. Bruhwiler, J. B. Miller, and M. Heimann, 2004. CH_4 sources estimated from atmospheric observations of CH_4 and its 13C/12C isotopic ratios:2. Inverse modeling of CH_4 fluxes from geographical regions. *Global Biogeochem. Cycles*, 18(GB4005): doi:10.1029/2004GB002224.

Miller, S.M., Wofsy, S.C., Michalak, A.M., Kort, E.A., Andrews, A.E., et al., 2013. Anthropogenic emissions of methane in the United States. *Proc. Nat'l Acad. Sci.*, 110:20018–20022, doi:10.1073/pnas.1314392110.

Nicolini, G., S. Castaldi, G. Fratini, and R. Valentini, 2013. A literature overview of micrometeorological CH_4 and N_2O flux measurements in terrestrial ecosystems. Atmospheric Environment, 81:311-319,doi:10.1016/j.atmosenv.2013.09.030.

Olson, D. M., T. J. Griffis, A. Noormets, R. Kolka, and J. Chen, 2013. Interannual, seasonal, and retrospective analysis of the methane and carbon dioxide budgets of a temperate peatland. *J. Geophys. Res. Biogeosci.*, *118*(1):226–238, doi:10.1002/jgrg.20031.

1044 Pelletier, L., T. R. Moore, N.T. Roulet, M. Garneau, and V. Beaulieu-Audy, 2007. Methane
1045 fluxes from three peatlands in the La Grande Rivière watershed, James Bay
1046 lowland, Canada. *J. Geophys. Res.*, 112(G01018): doi:10.1029/2006JG000216.
1047 Petrescu, A. M. R., J. van Huissteden, M. Jackowicz-Korczynski, A. Yurova, T. R.
1048 Christensen, P. M. Crill, K. Bäckstrand, and T. C. Maximov, 2007. Modelling
1049 CH_4 emissions from arctic wetlands: Effects of hydrological
1050 parameterization. *Biogeosciences*, 5:111–121, doi:10.5194/bg-5-111-2008.
1051 Petrescu, A.M.R., J. van Huissteden, M. Jackowicz-Korczynski, A. Yurova, T. R.
1052 Christensen, P. M. Crill, K. Backstrand, and T. C. Maximov, 2008. Modelling CH4
1053 emissions from arctic wetlands: effects of hydrological parameterization.
1054 *Biogeosciences*, 5: 111–121.
1055 Petrescu, A. M. R., L. P. H. van Beek, J. van Huissteden, C. Prigent, T. Sachs, C. A. R. Corradi,
1056 F. J. W. Parmentier, and A. J. Dolman, 2010. Modeling regional to global CH_4
1057 emissions of boreal and arctic wetlands, *Global Biogeochem. Cycles*,
1058 *24*(4):GB4009, doi:10.1029/2009GB003610.
1059 Potter, C.S. 1997. An ecosystem simulation model for methane production and emission
1060 from wetlands. *Global Biogeochem. Cycles*, 11:495–506.
1061 Potter, C.S., S. Klooster, S. Hiatt, M. Fladeland, V. Genovese, and P. Gross, 2006. Methane
1062 emissions from natural wetlands in the United States: Satellite-derived
1063 estimation based on ecosystem carbon cycling. *Earth Interactions*, 10(22):1-11.
1064 Pypker, T. G., P. A. Moore, J. M. Waddington, J. A. Hribljan, and R. C. Chimner, 2013.
1065 Shifting environmental controls on CH_4 fluxes in a sub-boreal peatland.
1066 *Biogeosciences*, *10*(12):7971–7981, doi:10.5194/bg-10-7971-2013.
1067 Reeburgh, W. S., J. Y. King, S. K. Regli, G. W. Kling, N. A. Auerbach, and D. A. Walker, 1998.
1068 A CH_4 emission estimate for the Kuparuk River basin, Alaska. *J. Geophys. Res.*, 103,
1069 29,005–29,013.
1070 Ridgwell, A. J., S. J. Marshall, and K. Gregson, 1999. Consumption of atmospheric
1071 methane by soils: A process-based model. *Global Biogeochem. Cycles*, 13(1):59–
1072 70, doi:10.1029/1998GB900004.
1073 Ringeval, B., N. De Noblet-Ducoudré, P. Ciais, P. Bousquet, C. Prigent, F. Papa, and W. B.
1074 Rossow, 2010. An attempt to quantify the impact of changes in wetland extent on
1075 methane emissions on the seasonal and interannual time scales, *Global*
1076 *Biogeochem. Cycles*, *24*(2):GB2003, doi:10.1029/2008GB003354.
1077 Rinne, J., T. Riutta, M. Pihlatie, M. Aurela, S. Haapanala, J. Tuovinen, E-S. Tuittila, and T.
1078 Vesala, 2007. Annual cycle of methane emission from a boreal fen measured by
1079 the eddy covariance technique. *Tellus B*, 59(3):449-457, doi:10.1111/j.1600-
1080 0889.2007.00261.x.
1081 Roulet, N.T., T. Moore, J. Bubier, and P. Lafleur, 1992. Northern fens: Methane flux and
1082 climate change. *Tellus B.*, 44:100-105.
1083 Sabrekov, A.F., B.R.K. Runkle, M.V. Galgolev, I.E. Kleptsova, and S.S. Maksyutov, 2014.
1084 Seasonal variability as a source of uncertainty in the West Siberian regional CH_4
1085 flux upscaling. *Environ. Res. Lett.*, 9:045008, doi:10.1088/1748-
1086 9326/9/4/045008.
1087 Sachs, T., C. Wille, J. Boike, and L. Kutzbach, 2008. Environmental controls on
1088 ecosystem-scale CH_4 emission from polygonal tundra in the Lena River Delta,
1089 Siberia. *J. Geophys. Res.*, 113(G00A03), doi:10.1029/2007JG000505.
1090 Salesky, S. T., M. Chamecki, and N. L. Dias, 2012. Estimating the random error in eddy-
1091 covariance based fluxes and other turbulence statistics: The filtering method.
1092 *Boundary-Layer Meteorol*, *144*(1):113–135, doi:10.1007/s10546-012-9710-0.

1093 Schrier-Uijl, A. P., P. S. Kroon, A. Hensen, P. A. Leffelaar, F. Berendse, and E. M.
1094 Veenendaal ,2010. Comparison of chamber and eddy covariance-based CO_2 and
1095 CH_4 emission estimates in a heterogeneous grass ecosystem on peat. *Agricultural*
1096 *and Forest Meteorology*, *150*(6):825–831, doi:10.1016/j.agrformet.2009.11.007.
1097 Shoemaker, J. K., T. F. Keenan, D. Y. Hollinger, and A. D. Richardson, 2014. Forest
1098 ecosystem changes from annual methane source to sink depending on late
1099 summer water balance. *Geophys. Res. Lett.*, 41:673–679,
1100 doi:10.1002/2013GL058691.
1101 Shurpali, N.J. and S.B. Verma. 1998. Micrometeorological measurements of methane flux
1102 in a Minnesota peatland during two growing seasons. *Biogeochem*., 40:1-15.
1103 Smeets, C., R. Holzinger, I. Vigano, A. Goldstein, and T. Röckmann, 2009. Eddy covariance
1104 methane measurements at a Ponderosa pine plantation in California.
1105 *Atmospheric Chemistry and Physics*, *9*(21):8365–8375, doi:10.5194/acp-9-8365-
1106 2009.
1107 Sonnentag, O., J. M. Chen, N. T. Roulet, W. Ju, and A. Govind, 2008. Spatially explicit
1108 simulation of peatland hydrology and carbon dioxide exchange: Influence of
1109 mesoscale topography. *J. Geophys. Res.*, *113*(G02005),
1110 doi:10.1029/2007JG000605.
1111 Spahni, R. *et al.,* 2011, Constraining global methane emissions and uptake by
1112 ecosystems, *Biogeosciences*, *8*(6):1643–1665, doi:10.5194/bg-8-1643-2011.
1113 Strack, M. and J.M. Waddington, 2007. Response of peatland carbon dioxide and
1114 methane fluxes to a water table drawdown experiment. *Global Biogeochem.*
1115 *Cycles*, 21(GB1007): doi:10.1029/2006GB002715.
1116 Strack, M., and J. M. Waddington, 2008. Spatiotemporal variability in peatland
1117 subsurface methane dynamics, *J. Geophys. Res.*, 113(G02010),
1118 doi:10.1029/2007JG000472.
1119 Sulman, B.N., A.R. Desai, B.D. Cook, N. Saliendra, and D.S. Mackay, 2009. Contrasting
1120 carbon dioxide fluxes between a drying shrub wetland in Northern Wisconsin,
1121 USA, and nearby forests. *Biogeosciences*, 6:1115-1126, doi:10.5194/bg-6-1115-
1122 2009.
1123 Sulman, B.N., A.R. Desai, and D. Mladenoff, 2013. Modeling soil and biomass carbon
1124 responses to declining water table in a wetland-rich landscape. *Ecosystems*,
1125 16:491-507, doi:10.1007/s10021-012-9624-1.
1126 Suyker, A. E., S.B. Verma, R.J. Clement, and D.P. Billesbach, D. P., 1996. Methane flux in a
1127 boreal fen: Season-long measurement by eddy correlation. *J. Geophys. Res.*
1128 101:28637-28647.
1129 Tagesson, T., M. Mölder, M. Mastepanov, C. Sigsgaard, M. P. Tamstorf, M. Lund, J. M. Falk,
1130 A. Lindroth, T. R. Christensen, and L. Ström, 2012. Land-atmosphere exchange of
1131 methane from soil thawing to soil freezing in a high-Arctic wet tundra ecosystem.
1132 *Global Change Biol*, *18*(6):1928–1940, doi:10.1111/j.1365-2486.2012.02647.x.
1133 Tang, J., Q. Zhuang, R. D. Shannon, and J. R. White, 2010. Quantifying wetland methane
1134 emissions with process-based models of different complexities. *Biogeosciences*,
1135 *7*(11):3817–3837, doi:10.5194/bg-7-3817-2010.
1136 Tian, HQ, X. Xu, M. Liu, W. Ren, C. Zhang, G. Chen, and C. Lu. 2010. Spatial and temporal
1137 patterns of CH_4 and N_2O fluxes in terrestrial ecosystems of North America during
1138 1979–2008: application of a global biogeochemistry model, *Biogeosciences 7*,
1139 2673-2694.
1140 Turetsky, M. R., C. C. Treat, M. P. Waldrop, J. M. Waddington, J. W. Harden, and A. D.
1141 Mcguire, 2008. Short-term response of methane fluxes and methanogen activity

to water table and soil warming manipulations in an Alaskan peatland. *J. Geophys Res*, *113*:G00A10, doi:10.1029/2007JG000496.
Ullah, S., and T. R. Moore, 2011. Biogeochemical controls on methane, nitrous oxide, and carbon dioxide fluxes from deciduous forest soils in eastern Canada. *J. Geophys Res*, *116*:G3010, doi:10.1029/2010JG001525.
van Huissteden, J., T. C. Maximov, and A. J. Dolman, 2005. High methane flux from an arctic floodplain (Indigirka lowlands, eastern Siberia). *J. Geophys. Res.*, 110:G02002, doi:10.1029/2005JG000010.
van Huissteden, J, A.M.R. Petrescu, D.M.D. Hendriks, and K.T. Rebel, 2009. Sensitivity analysis of a wetland methane emission model based on temperate and arctic wetland sites. *Biogeosciences* 6:3035-3051, doi:10.5194/bg-6-3035-2009.
Waddington, J., and S. Day, 2007. Methane emissions from a peatland following restoration. *J. Geophys Res*., 112:G03018, doi:10.1029/2007JG000400.
Walter B.P. and M. Heimann M., 2000. A process-based, climate- sensitive model to derive methane emissions from natural wetlands: application to five wetland sites, sensitivity to model parameters, and climate. *Global Biogeochem. Cycles* 14:745–765.
Walter, B.P., M. Heimann, and E. Matthews, 2001. Modeling modern methane emissions from natural wetlands: 2. Interannual variations 1982-1993. *J. Geophys. Res.*, 106:34207-34219, doi:10.1029/2001JD900164.
Wang, W., K.J. Davis, D.M. Ricciuto, and M.P. Butler, 2006. An approximate footprint model for flux measurements in the convective boundary layer. *Journal of Atmospheric and Oceanic Technology*, 23:1384-1394.
Webb, E.K., G.I. Pearman, and R. Leuning, 1980. Correction of flux measurements for density effects due to heat and water vapor transfer. *Quart. J. Roy. Meteorol. Soc.*, 106, 85-100.
Weishampel, P. and R. K. Kolka, 2008. Measurement of methane fluxes from terrestrial landscapes using static, non-steady state enclosures. In C. M. Hoover (editor) *Field Measurements for Forest Carbon Monitoring: A Landscape Scale Approach*. Springer, New York, NY.
Werner, C., K.J. Davis, P. Bakwin, C. Yi, D. Hurst, and L. Lock, 2003. Regional-scale measurements of CH_4 exchange from a tall tower over a mixed temperate/boreal lowland and wetland forest. *Global Change Biology*, 9:1251-1261.
Whiting G. J. and Chanton J. P., 1993. Primary production control of methane emission from wetlands. *Nature* 364, 794 – 795.
Wille, C., L. Kutzbach, T. Sachs, D. Wagner, and E-M. Pfeiffer, 2008. Methane emission from Siberian arctic polygonal tundra: eddy covariance measurements and modeling . *Global Change Biology*, 14: 1395-1405, doi: 10.1111/j.1365-2486.2008.01586.x.
Xu, X.F., H.Q. Tian, C. Zhang, M.L. Liu, W. Ren, G.S. Chen, C.Q. Lu, and L. Bruhwiler, 2010. Attribution of spatial and temporal variations in terrestrial methane flux over North America. *Biogeosciences* 7:3637–55, doi:10.5194/bg-7-3637-2010.
Yu, J., W. Sun, J. Liu, J. Wang, J. Yang, and F. X. Meixner, 2007. Enhanced net formations of nitrous oxide and methane underneath the frozen soil in Sanjiang wetland, northeastern China. *J. Geophys. Res.*, 112(D07111): doi:10.1029/2006JD008025.
Yu, L., H. Wang, G. Wang, W. Song, Y. Huang, S.-G. Li, N. Liang, Y. Tang, and J.-S. He, 2013. A comparison of methane emission measurements using eddy covariance and manual and automated chamber-based techniques in Tibetan Plateau alpine wetland. *Environmental Pollution*, *181*:81–90, doi:10.1016/j.envpol.2013.06.018.

1191 Zhang, Y., C. Li, C.C. Trettin, H. Li, and G. Sun, 2002. An integrated model of soil,
1192 hydrology, and vegetation for carbon dynamics in wetland ecosystems. *Global*
1193 *Biogeochem. Cycles*, 16(4, 1061), doi:10.1029/2001GB001838.
1194 Zhang, Y., Sachs, T., Li, C. and Boike, J., 2012. Upscaling methane fluxes from closed
1195 chambers to eddy covariance based on a permafrost biogeochemistry integrated
1196 model. *Global Change Biology*, 18:1428–1440, doi: 10.1111/j.1365-
1197 2486.2011.02587.x.
1198 Zhuang Q., A.D. McGuire, P.A. Steudler, B.S. Felzer, S. Hu, J.M. Melillo, D.W. Kicklighter,
1199 and R.G. Prinn, 2004. Methane fluxes between terrestrial ecosystems and the
1200 atmosphere at northern high latitudes during the past century: A retrospective
1201 analysis with a process-based biogeochemistry model. *Global Biogeochem. Cycles*,
1202 18(GB3010):1-23.

1203 # Tables

1204 **Table 1.** Very tall tower site and instrument characteristics

Coordinates	45.945^{o} N, 90.273^{o} W
Land cover (general region)	28% wetland, 67% upland mixed forest, 5% grass or other
Mean annual temperature (1995-2013)	5.7 C
Annual precipitation (1995-2013)	586 mm
Summer temperature (JJA, 1995-2013)	18.4 C
Summer precipitation (JJA, 1995-2013)	243 mm
Measurement height	122 m above ground for CH_4; 30, 122 and 396 m for CO_2, H_2O, heat and momentum
Instruments	
Flux gas analyzer (CH_4)	Picarro, Inc. 1301-f
Flux gas analyzer (CO_2/H_2O)	Licor, Inc. LI-6262
Storage profile (CH_4)	Los Gatos, Inc. LGR Fast Methane Analyzer
Storage profile (CO_2)	Licor, Inc. LI-7000
Sonic anemometer	ATI, Inc. Type K
u* cutoff	0.2 m s^{-1}

1205
1206

1207 **Table. 2** DLEM model gridcell cover fractions

Plant functional type	DLEM Regional (%)	DLEM Site (%)
Wetland	44	28
Forest	43	67
Grass and other	13	5

1208
1209

1210 **Table 3.** Observed annual fluxes and meteorology during study period

	2011	*2012*
Annual mean temperature (degrees C)	5.7	7.0
Annual precipitation (mm)	458	568
Summer (JJA) temperature (degrees C)	19.1	19.4
Summer (JJA) precipitation (mm)	207	188
NEE CO_2 (gC-CO_2 m^{-2} yr^{-1})	-58.0	-101.4
GPP (gC-CO_2 m^{-2} yr^{-1})	858.1	1160.7
R_{eco} (gC-CO_2 m^{-2} yr^{-1})	799.7	1059.3
NEE CH4 (mgC –CH_4 m^{-2} yr^{-1})	911 +/- 84	659 +/- 64
Ratio NEE CH_4:NEE CO_2 (%)	-1.57	-0.65
Ratio NEE CH_4:R_{eco} (%)	0.0011	0.00062
Missing NEE CH_4 (%)	29	36
Screened NEE CH_4 (%)	12	13

1211
1212

Table 4. Pearson linear correlation coefficient (r) between NEE CH_4 and other observations at hourly to monthly averaging scales. Only significant correlations ($p<0.1$) are shown after correcting for time series auto-correlation. NEE CH_4 is not strongly correlated to soil moisture, but instead most positively correlated to temperature and GPP and R_{eco} at these time scales.

Averaging Time	Temperature	Photo-syn-thetic-ally active rad-iation (PAR)	Volumetric surface soil moisture	Net ecosystem exchange CO_2 (NEE CO_2)	Gross primary production (GPP)	Ecosystem respiration (R_{eco})
Hour				0.09		
Day	0.49	0.43			0.49	0.53
Week	0.71	0.66		-0.49	0.72	0.74
Month				-0.68	0.80	0.79

Figures

Figure 1. Generalized land cover surrounding the WLEF Park Falls very tall tower (center cross) in a 10 km radius derived from manual classification of 30 m spatial resolution 2004 Quickbird imagery (B.D. Cook, unpublished data). "Other" category primarily includes grassy areas, lakes, and streams. Wetlands are patchy and equally distributed in all directions from tower. Footprint climatology overlaid as a mask, where lighter areas show > 0.5% contribution to the May-Sept 2011 total hourly surface flux influence, revealing a typical footprint diameter of 5 km.

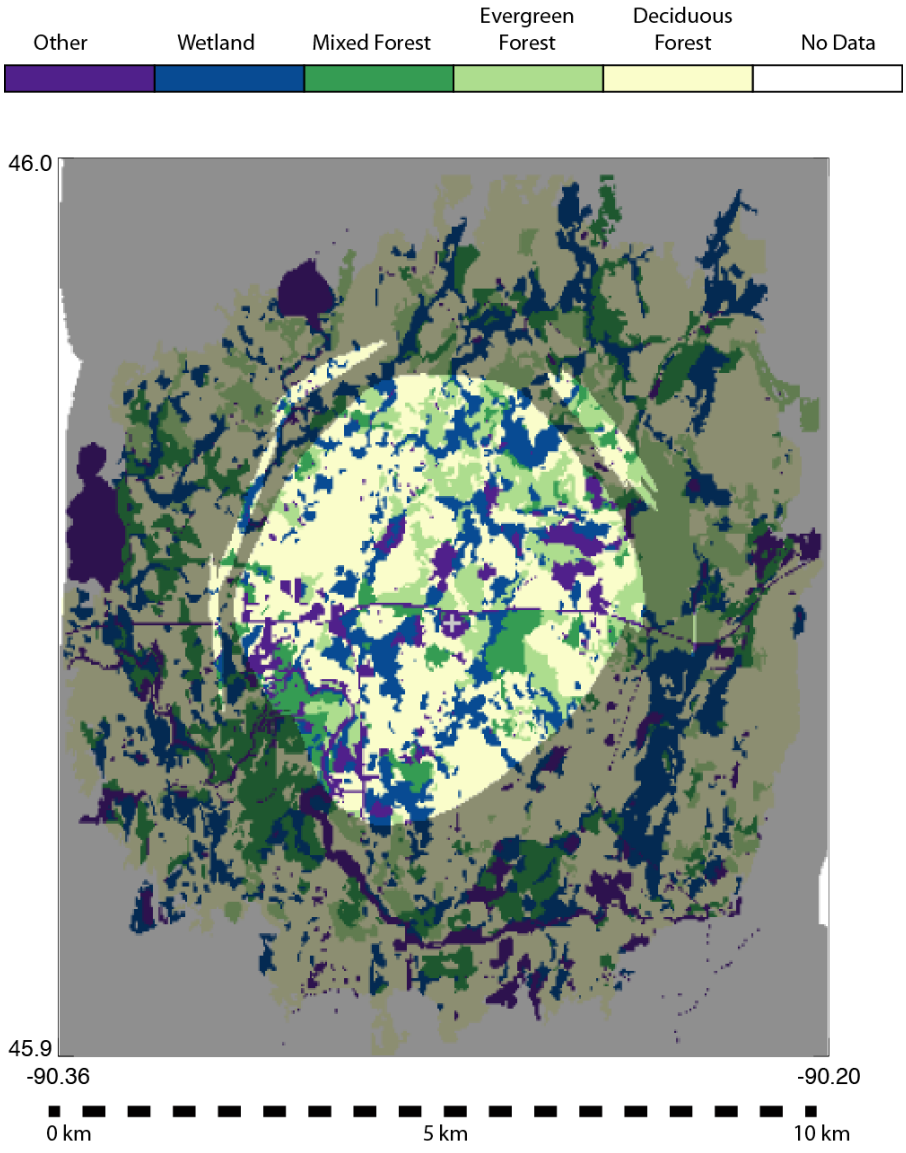

Figure 2. Comparison of in-line water vapor correction and post-WPL correction for water vapor dilution applied to CH_4 eddy fluxes. a) Comparison of "wet" mole fraction CH_4 flux to "wet" mole fraction CH_4 flux with WPL applied, showing the effect of water vapor dilution is to underestimate fluxes by ~1%. b) A direct dry mole fraction estimated flux shows high correlation and low bias with WPL-corrected CH_4 flux, but the direct computed fluxes are on average 1.6% larger.

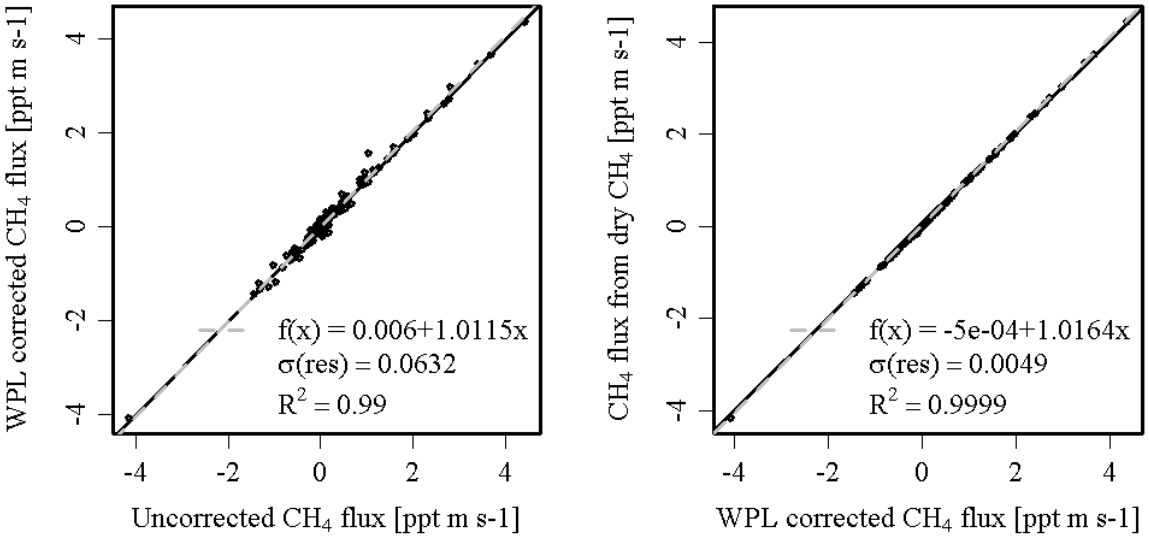

Figure 3. Estimate of flux random turbulent uncertainty (y-axis) versus absolute magnitude of NEE CH_4 for a) hourly and b) daily scale. The blue line shows bin-averaged NEE CH_4 for intervals of a) 10 nmol CH_4 m^{-2} s^{-1} or b) 4 mg C-CH_4 m^{-2} day^{-1}, while the red line shows the result of linear regression. In general, uncertainty scales linearly with flux. The intercept is an estimate of minimal detectable flux.

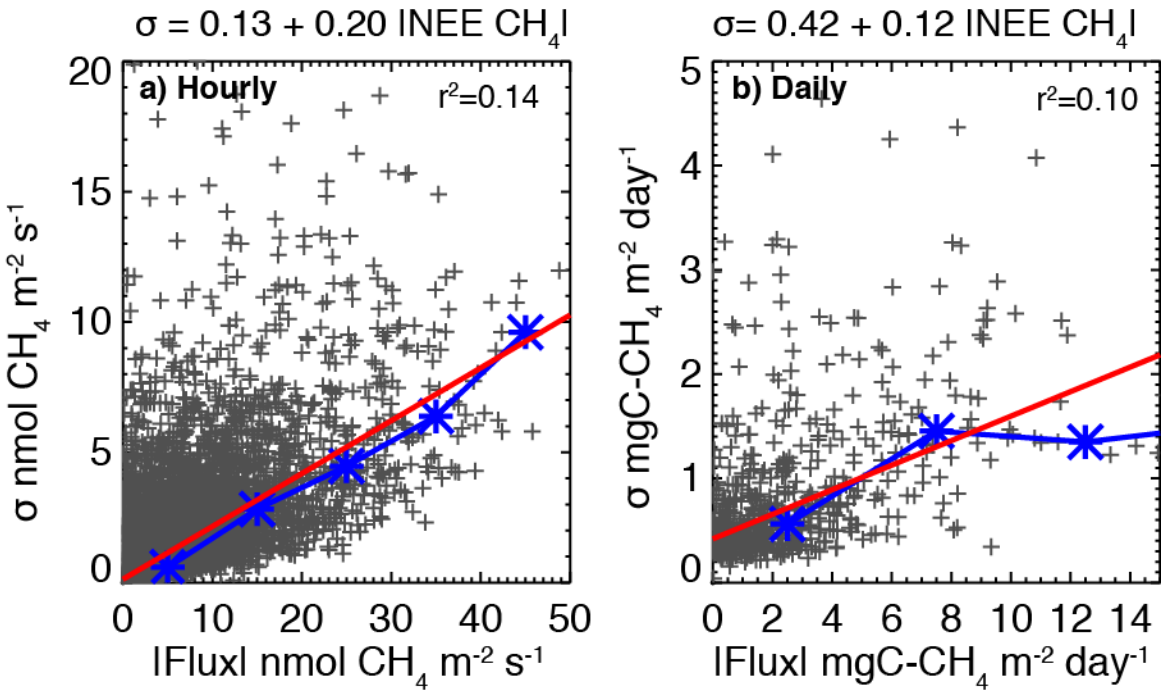

Figure 4. a) Box plot comparing the range of NEE CH_4 observed from soil chamber observations made at four wetlands (first four from left) and three uplands forests from April-October 2005-2006 compared to the eddy flux tower hourly observations in 2011-2012. Number of observations for each measurement is listed below the site abbreviation on the x-axis. b) The comparison of monthly NEE CH_4 from the tower averaged over 2011-2012 (black bars) and the profile-based Modified Bowen ratio approach of Werner *et al*. (2003) for 1998 (red bars). Site to site variability in chamber wetland fluxes was high but was bracketed by the tower based regional flux estimates. Regional flux estimates from the Bowen ratio approach were in general much larger than those estimated from tower, despite similar climates in 1998 and 2011-2012. .

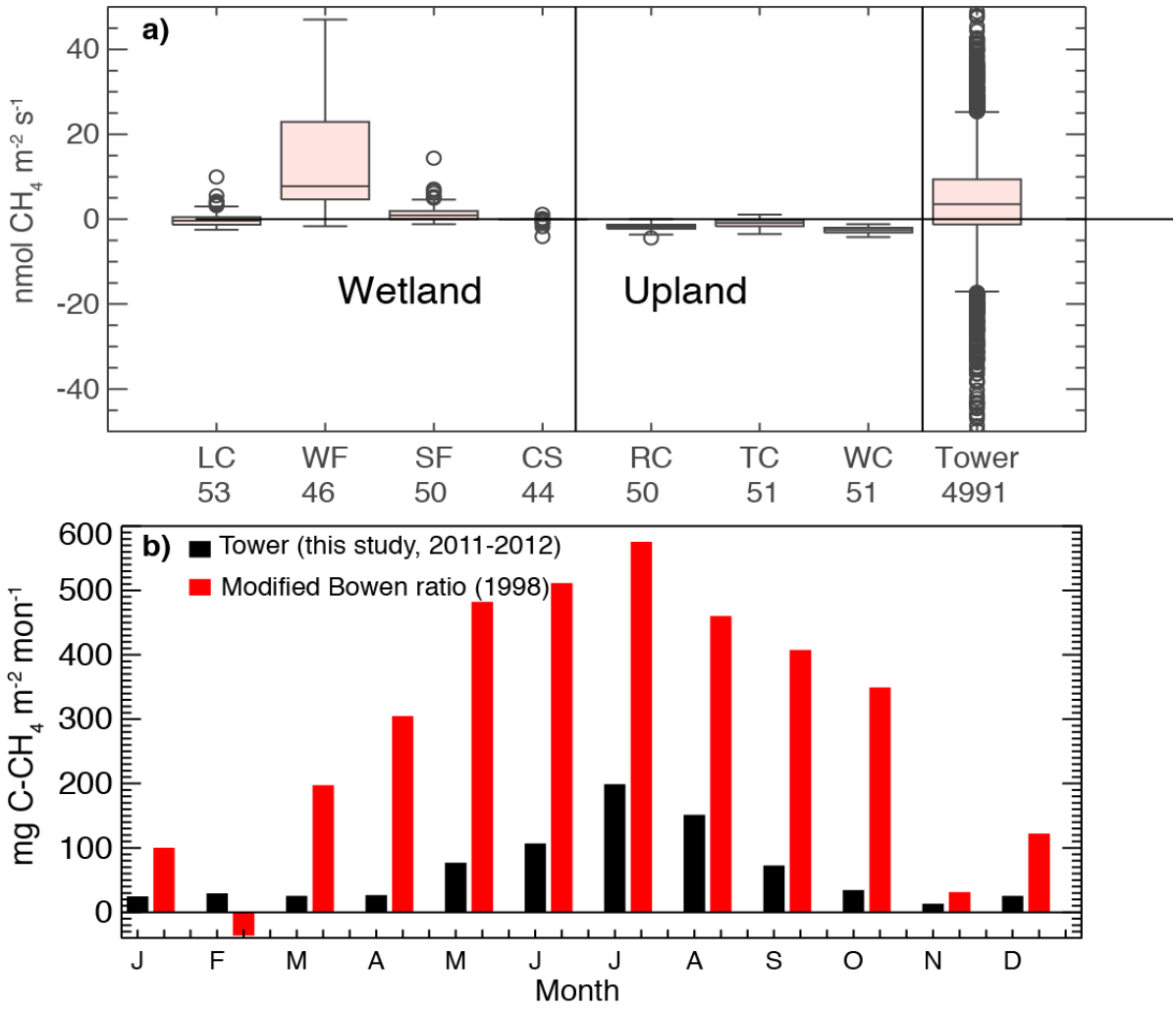

Figure 5. Time series of daily a) NEE of CH_4, b) NEE of CO_2, c) GPP and d) R_{eco} for a two-year period at the tower site. Red crosses are gap-filled, and gray bars show turbulent flux uncertainty. Blue line shows a 10 day smoothed average. CH_4 fluxes show a decline from 2011 to 2012 in contrast to increases seen in GPP and R_{eco} and no change in NEE.

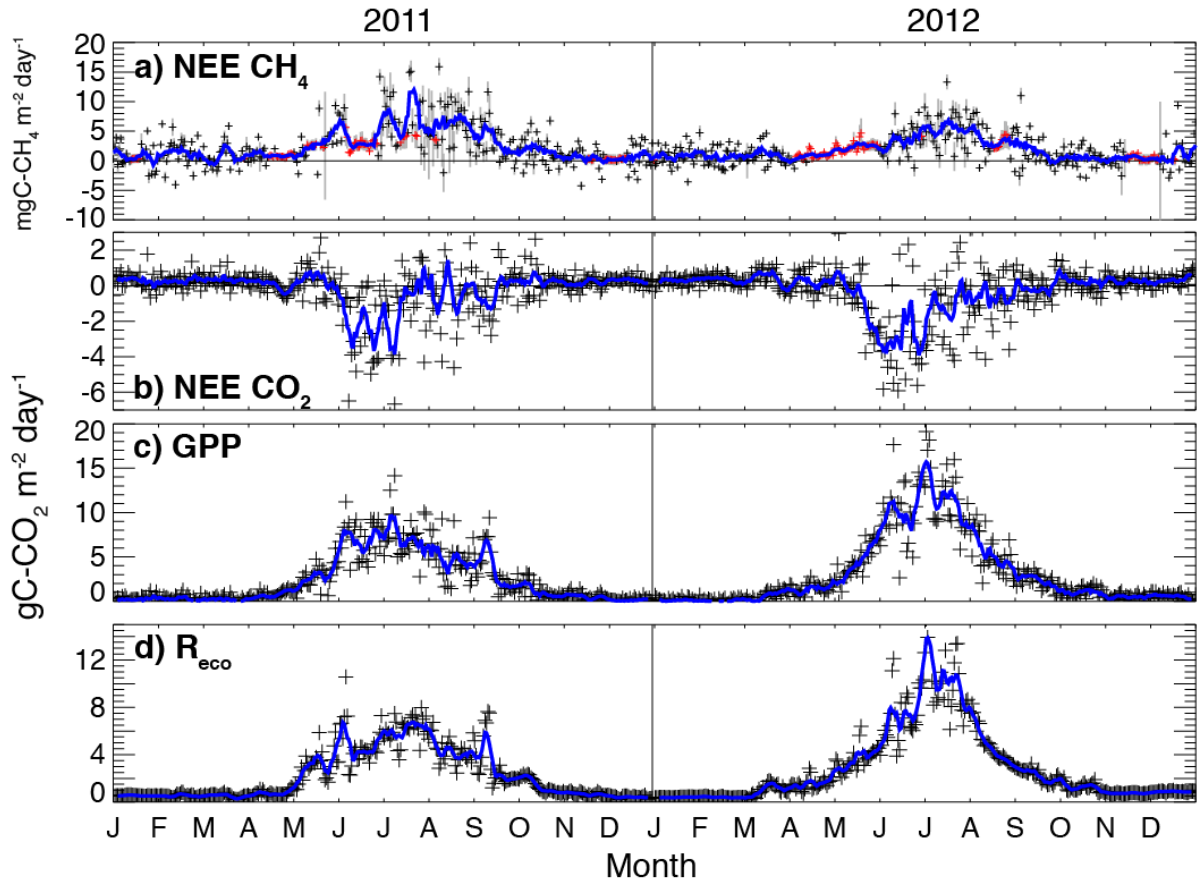

Figure 6. Similar to Figure 5 but for meteorological forcing of gap-filled a) daily mean temperature, b) daily cumulative photosynthetically active radiation, c) cumulative precipitation, and d) near surface soil moisture from an upland, mixed forest in the flux tower footprint. Both years had similar temperature and cloudiness, but differing patterns of growing season precipitation leading to lower soil moisture available in 2012.

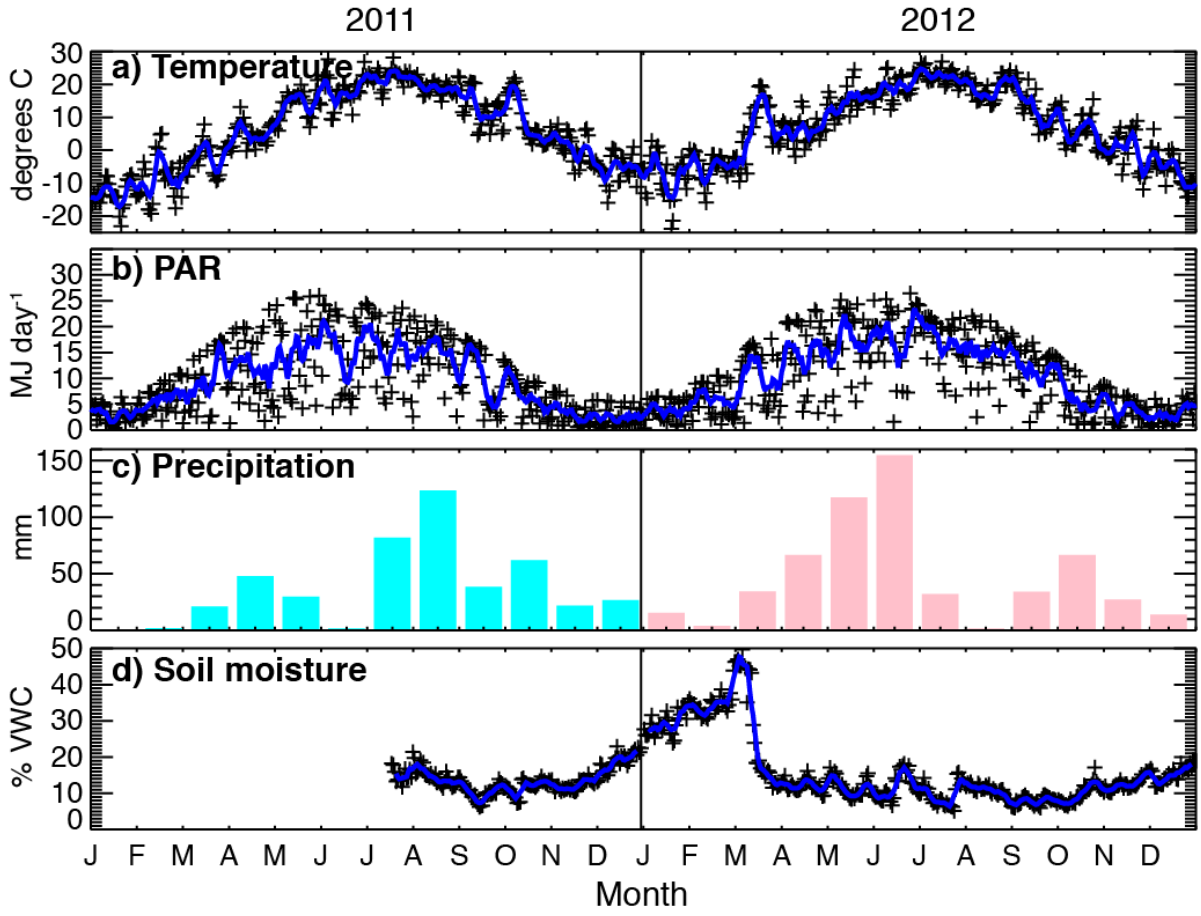

Figure 7. a) Cumulative NEE of CH_4 for 2011 (blue) and 2012 (red) and estimate of cumulative flux uncertainty. NEE from the two years diverges at the start of the growing season, but cannot be differentiated against flux uncertainty until the end of the growing season. b) Normalized Hilbert-Huang transformed (HHT) power spectra of NEE CH_4 (red) and NEE CO_2 (black) show that modes of variability in cumulative flux are similar for the two, though CO_2 has a clearer spectral gap between diurnal/synoptic and seasonal/annual variations, while CH_4 has stronger monthly variations and weaker seasonal contributions.

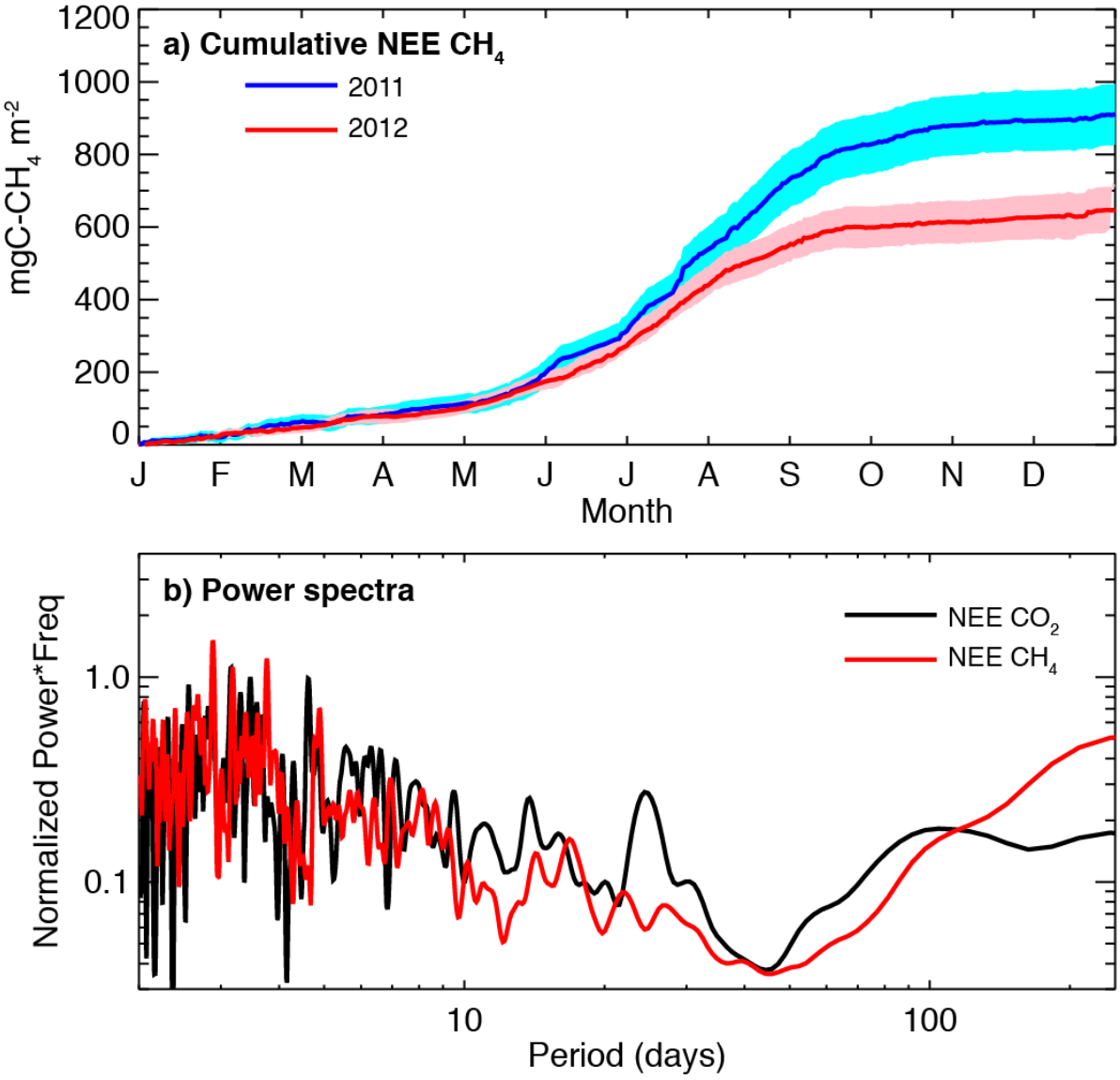

Figure 8. Diel patterns of a) NEE CH_4, b) NEE CO_2, c) GPP, and d) R_{eco} for the summer season (June-August) for 2011 (blue) and 2012 (red). Bands shaded blue and pink reflect standard deviation of flux for that hour. NEE CH_4 has an unusual minimum of mid-morning flux, followed in succession by NEE CO_2 (late-morning), GPP (noon), and R_{eco} (afternoon). R_{eco} and NEE CH_4 show clearest changes in mean fluxes between 2011 and 2012.

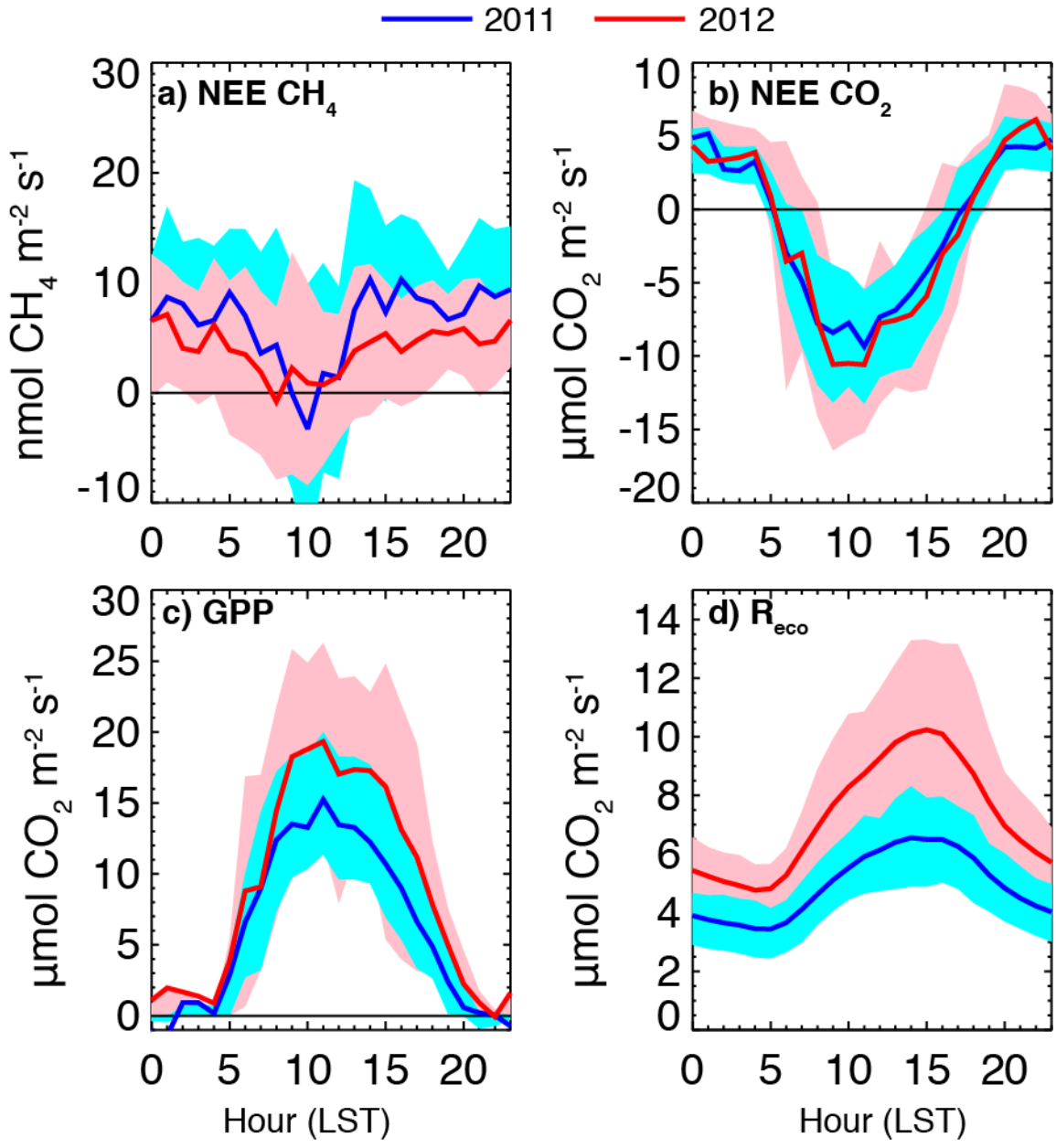

Figure 9. Scatterplot relationships of NEE CH_4 (black dots) at hourly (left) and daily (right) scales to GPP (top) and air temperature (bottom) including accounting for uncertainty (gray bars). A linear model best reflects relationship to GPP, while an exponential model is used for temperature. Fluxes shown with uncertainty, and fit (red line) shown with random propagation of 2-σ uncertainty in parameters of fit.

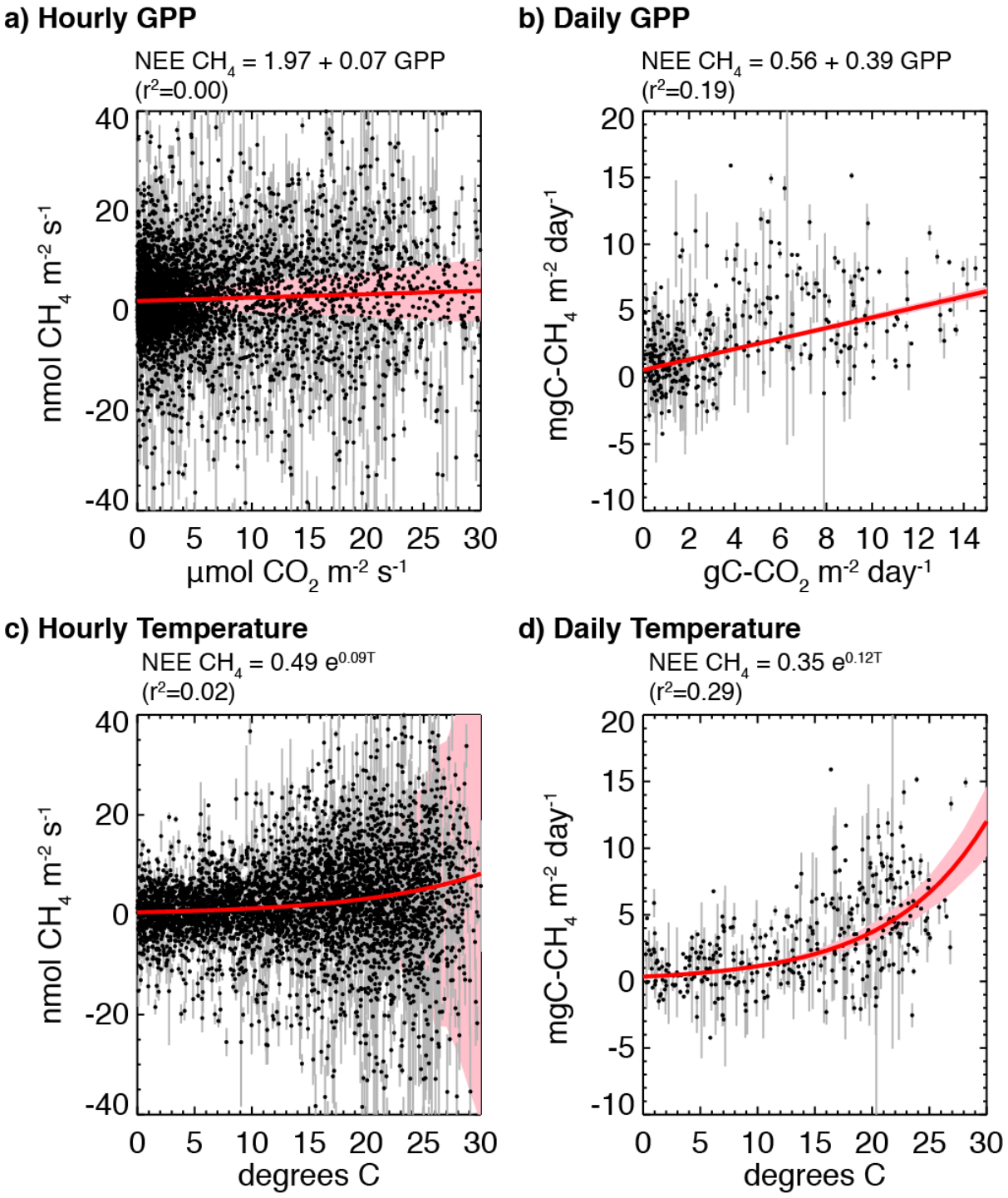

Figure 10. Comparison of daily (cross) NEE CH_4 and uncertainty (gray bars) to simulations of the DLEM model from a cut-out from a larger regional model (blue line, only for 2012) and a locally forced model with accounting of sub-grid land cover (red line, both years). Pink crosses reflect gap-filled observations. Both models were able to capture the seasonal cycle of CH_4 flux, but the site model more faithfully reproduced mean flux at expense of underestimating large positive excursions of flux and not capturing reduction of flux in 2012.

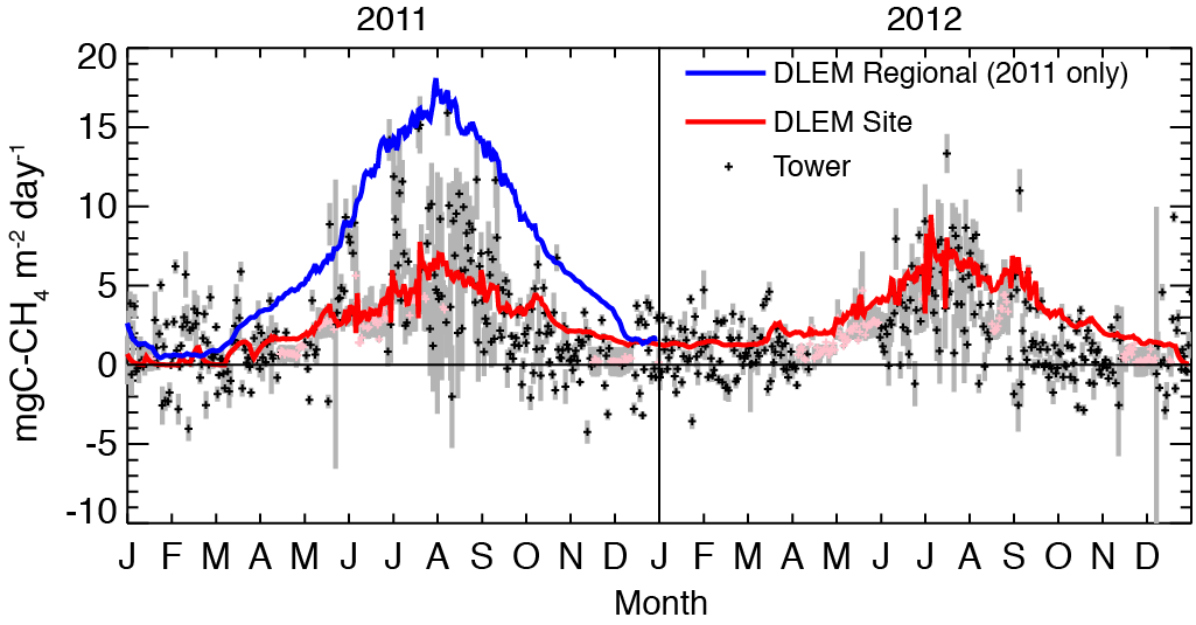

Figure S1. Profiles of CH_4 (left) and CO_2 (right) concentration (top) at 30 (black), 122 (blue), and 396 m (red) level and CH_4 and CO_2 net ecosystem exchange (black), turbulent flux (red), and storage flux (blue) at 122 m (bottom).